

**PHYSICAL MODEL STUDY OF THE EFFECTS OF WETTABILITY AND  
FRACTURES ON GAS-ASSISTED GRAVITY DRAINAGE (GAGD)  
PERFORMANCE**

A Thesis

Submitted to the Graduate Faculty of the  
Louisiana State University and  
Agricultural and Mechanical College  
in partial fulfillment of the  
requirements for the degree of  
Master of Science in  
Petroleum Engineering

In

The Department of Petroleum Engineering

by  
Wagirin Ruiz Paidin  
B.S., Anton De Kom University of Suriname, 2001  
May 2006

## **ACKNOWLEDGEMENTS**

I am thankful to Dr. Rao for his unwavering belief in me and the wisdom to give me the space and freedom to do my research work, and to Dr. White and Dr. Langlinais for graciously agreeing to serve on my exam committee. Also, I would like to thank all my lab mates for their technical help during the project.

I am indebted to the Organization of American States and LASPAU for providing me with the financial support and the opportunity to study at the Louisiana State University. A final word of gratitude is reserved for my friends and family who have always provided me with their unending support and love.

## TABLE OF CONTENTS

ACKNOWLEDGEMENTS .....	ii
LIST OF TABLES .....	v
LIST OF FIGURES .....	vi
NOMENCLATURE .....	viii
ABSTRACT .....	ix
CHAPTER 1. INTRODUCTION .....	1
1.1 Objective .....	1
1.2 Methodology .....	1
CHAPTER 2. LITERATURE REVIEW .....	3
2.1 Enhanced Oil Recovery (EOR) Methods .....	3
2.1.1 Introduction .....	3
2.1.2 Types of EOR .....	5
2.2 The Development of the Gas-Assisted Gravity Drainage (GAGD) Process .....	6
2.2.1 Introduction .....	6
2.2.2 The Concept behind the GAGD Process .....	6
2.2.3 Developments in Horizontal Drilling .....	7
2.3 The Effect of Wettability on Oil Recovery .....	8
2.3.1 Introduction .....	8
2.3.2 Spreading .....	11
2.3.3 Fluid Displacement Energy .....	11
2.3.4 Wettability and Oil Recovery – Waterfloods .....	12
2.3.5 Wettability and Oil Recovery – Gas Injection .....	13
2.4 Determination of the Wettability .....	15
2.4.1 The Contact Angle .....	16
2.4.2 The Amott Method .....	17
2.5 The Alteration of the Wettability of the Glass Beads through Silylation .....	18
2.5.1 Introduction .....	18
2.5.2 The Silylation Reaction Mechanism .....	18
2.6 Fracture Simulation within the GAGD Process .....	20
2.6.1 Literature Review .....	20
2.6.2 Fracture Simulation .....	21
2.7 Scaling Groups for Experimental Set-up .....	21
2.7.1 Introduction .....	21
2.7.2 Dimensionless Groups .....	23
CHAPTER 3. EXPERIMENTAL APPARATUS AND PROCEDURE .....	26
3.1 Task Formulation .....	26
3.2 Chemicals and Reagents .....	26
3.3 Apparatus .....	28

3.4 Experimental Procedure.....	29
3.4.1 Procedure for the Alteration of the Wettability of Glass Beads Using Dimethyldichlorosilane.....	29
3.4.2 Simplified Procedure for the Wettability Alteration of Glass Beads Using Dimethyldichlorosilane.....	30
3.4.3 Modified Procedure for the Amott Test.....	31
3.4.4 Preparation of the Pistoned Transfer Vessel.....	32
3.4.5 Preparing the Porous Medium.....	33
3.4.6 Initiating the Gas Displacement Experiments.....	34
3.4.7 Procedure for Conducting the Secondary Displacement Experiments.....	34
3.4.8 Procedure for Conducting the Tertiary Displacement Experiments.....	35
3.5 Overview of the Conducted Experiments.....	36
 CHAPTER 4. RESULTS AND DISCUSSION.....	 40
4.1 The Confirmation of the Wettability Alteration.....	40
4.2 The Effect of Wettability on GAGD Performance.....	42
4.2.1 The Secondary Mode Gas Displacement Experiments.....	42
4.2.1.1 Discussion of the Results.....	42
4.2.2 The Tertiary Mode Gas Displacement Experiments.....	48
4.2.2.1 The Experimental Results.....	48
4.2.2.2 Discussion of the Results.....	48
4.3 The Experiments Simulating a Fracture.....	52
4.3.1 The Results.....	52
4.3.2 Discussion of the Results.....	53
4.4 The Dimensionless Groups.....	62
4.4.1 The Bond Number.....	63
4.4.2 The Capillary Number.....	64
4.4.3 Statistical Analysis of the Results.....	64
 CHAPTER 5. CONCLUSIONS AND RECOMMENDATIONS.....	 69
5.1 Summary of Findings and Conclusions.....	69
5.2 Recommendations for Future Work.....	70
 REFERENCES.....	 71
 VITA.....	 73

## LIST OF TABLES

2.1. Estimated Annual Worldwide Production of Oil by EOR circa January 1992 (Lake, 1992) .....	4
3.1. Particle Size Distribution Silica Sand (downloaded from U.S. Silica website).....	28
4.1. Model Parameters for the Water-Wet Runs in Secondary Mode .....	45
4.2. Model Parameters for the Oil-Wet Runs in Secondary Mode – Constant Pressure Runs .....	45
4.3. Model Parameters for the Oil-Wet Runs in Secondary Mode – Constant Flow Rate Runs .....	46
4.4. Model Parameters for the Tertiary Mode Water – Wet Runs .....	51
4.5. Model Parameters for the Tertiary Mode Oil – Wet Runs.....	52
4.6. Summary of Incremental Effect of the Wettability on the Oil Recovery .....	54
4.7. Model Parameters for the Fracture Simulation Runs.....	56
4.8. Summary of the Incremental Effect of the Fracture on the Oil Recovery .....	56
4.9. Summary of the Incremental Effect of the Wettability on the Fractured Runs .....	60
4.10. Experimental GAGD Results of Sharma (2005) – Secondary Mode .....	66

## LIST OF FIGURES

2.1. Overview of Oil Recovery Mechanisms (Lake, 1992) .....	4
2.2. The Concept behind the GAGD Process (Rao et al., 2004).....	7
2.3. Physical Model with Vertical Fracture Simulation.....	22
3.1. Reaction Mechanism of the Wettability Alteration Procedure .....	31
3.2. Schematic Diagram of Experimental Setup.....	33
4.1. Visual Comparison of Water-Wet Porous Medium (Left) with Oil-Wet Porous Medium (Right) During Oil Flooding .....	41
4.2. Fractional Flow Curves for the 0.13 mm Silica Sand.....	43
4.3. Fractional Flow Curves for the 0.15 mm Glass Beads .....	43
4.4. Effect of the Injected Gas on the Oil Recovery – Secondary Mode Runs.....	46
4.5. Effect of the Gas Injection Method on the Oil Recovery – Secondary Mode Runs, Oil-Wet Case, 0.13 mm Sand Pack .....	47
4.6. Effect of Average Grain Size on the Oil Recovery – Secondary Mode Runs .....	49
4.7. Effect of the Wettability on the Oil Recovery – Secondary Mode, Constant Pressure, 0.13 mm Sand Pack .....	49
4.8. Effect of the Wettability on the Oil Recovery – Secondary Mode, Constant Pressure, 0.15 mm Glass Bead Pack .....	50
4.9. Effect of the Wettability on the Oil Recovery – Secondary Mode, Constant Rate, 0.13 mm Sand Pack .....	50
4.10. Effect of Gas Injection Method on the Oil Recovery – Tertiary Mode Runs.....	53
4.11. Effect of the Wettability on the Oil Recovery – Tertiary Mode, 0.15 mm Glass Bead Pack .....	55
4.12. Effect of the Wettability on the Oil Recovery – Tertiary Mode, 0.13 mm Sand Pack .....	55
4.13. Effect of a Vertical Fracture on the Oil Recovery – Water-Wet Case, 0.13 mm Sand Pack .....	57
4.14. Gas Injection Profile into Water-Wet Fracture Simulation – 0.13 mm .....	58

4.15. Effect of a Vertical Fracture on the Oil Recovery – Water-Wet Case, 0.15 mm Glass Bead Pack .....	58
4.16. Regions Bypassed by N-Decane Flood in Fracture Simulation – Water-Wet, 0.15 mm.....	59
4.17. Effect of a Vertical Fracture on the Oil Recovery – Oil-Wet Case, 0.13 mm Sand Pack .....	59
4.18. Effect of a Vertical Fracture on the Oil Recovery – Oil-Wet Case, 0.15 mm Glass Bead Pack .....	60
4.19. Effect of the Wettability on Fractured Runs – 0.13 mm Sand Pack .....	61
4.20. Effect of the Wettability on Fractured Runs – 0.15 mm Glass Bead Pack .....	61
4.21. Effect of Grain Size on Recovery in Fractured Model – Water-Wet Runs .....	65
4.22. Effect of Grain Size on Recovery in Fractured Model – Oil-Wet Runs .....	65
4.23. The Relation between the Bond Number and Oil Recovery.....	66
4.24. The Relation between the Capillary Number and Oil Recovery .....	67
4.25. Similarities between the Capillary Number Trends.....	67
4.26. Multiple Regression Analysis Results for the Secondary Mode Experiments .....	68
4.27. Multiple Regression Analysis Results for the Tertiary Mode Experiments .....	68

## NOMENCLATURE

$D$  = the grain size diameter

$g$  = the gravitational acceleration

$g_c$  = a gravitational acceleration conversion factor

$h$  = the height of the porous medium

$K$  = the absolute permeability of the porous medium

$l$  = a characteristic length of the porous medium

$N_B$  = the Bond number

$N_C$  = the capillary number

$N_G$  = the gravity number

$P$  = the pressure

$R_a$  = the average pore throat radius

$S_{or}$  = the residual oil saturation

$S_{wi}$  = the initial water saturation

$S_{wr}$  = the residual water saturation

$t$  = the injection time

$V_{osp}$  = the oil volume displaced by spontaneous imbibition of water

$V_{ot}$  = the total oil volume displaced by imbibition and forced displacement

$V_{wsp}$  = the water displaced by spontaneous oil imbibition alone

$V_{wt}$  = the total volume of water displaced by oil imbibition and forced displacement

$Z$  = the average position of the gas interface

$\sigma$  = interfacial tension between the two fluids

$\Delta\rho$  = the density difference between the two fluids

$\delta_o$  = the displacement-by-oil ratio

$\delta_w$  = the displacement-by-water ratio

$\phi$  = the porosity of the porous medium

$\mu$  = the viscosity of the oleic phase

$v$  = the Darcy velocity

$\theta$  = the contact angle

$\tau$  = the tortuosity of the flow path through the porous medium

## ABSTRACT

The Gas-Assisted Gravity Drainage (GAGD) process was developed to take advantage of the natural segregation of injected gas from crude oil in the reservoir. It consists of placing a horizontal producer near the bottom of the reservoir and injecting gas using existing vertical wells. As the injected gas rises to the top to form a gas cap, oil and water drain down to the horizontal producer. Earlier experimental work using a physical model by Sharma had demonstrated the effectiveness of the GAGD process in improving the oil recovery when applied in water-wet porous media. The current research is an extension of that work and is focused on evaluating the effect of the wettability of the porous medium and the presence of a vertical fracture on the GAGD performance. The effect of the injection strategy (secondary and tertiary mode) on the oil recovery was also evaluated in the experiments. In the physical model experiments a Hele-Shaw type model was used (dimensions: 13 7/8" by 5/16" by 1") along with glass beads and silica sand as the porous media. Silanization with an organosilane (dimethyldichlorosilane) was used to alter the wettability of the glass beads from water-wet to oil-wet.

The experiments showed a significant improvement of the oil recovery in the oil-wet experiments versus the water-wet runs, both in the secondary and the tertiary modes. The fracture simulation experiments have also shown an increase in the effectiveness of the GAGD process.

# CHAPTER 1

## INTRODUCTION

### 1.1 Objective

The effect of the wettability of the porous medium on the performance of the Gas-Assisted Gravity Drainage (GAGD) has not yet been evaluated in the past, even though the GAGD process was essentially developed to be applicable to all types of oil reservoirs. It is generally assumed that most oil reservoirs are water-wet because water is the medium in which the particulate material that makes up the source material for reservoir quality rock is deposited. Previous research on the GAGD process involved the use of water-wet glass beads as the porous medium in a physical model. The effect of physical (the mode of gas injection, the strategy of gas injection, and the type of gas injected) and dimensionless (the Bond and capillary numbers) parameters on the performance was the broad aim in previous research (Sharma, 2005). It is expected that the GAGD process will perform better in oil-wet reservoirs because of the continuity of oil films throughout an oil-wet porous medium even at very low oil saturations.

The objective of this study is to investigate the effect of certain (petro)physical parameters on the performance of the GAGD process, namely the wettability of the porous medium and the presence of a vertical fracture in the porous medium.

### 1.2 Methodology

In the present study, several gas displacement experiments were conducted to study the effects of wettability and fractures on the performance of the GAGD process. In the experiments, n-decane and deionized water were used as the fluids in gas displacement runs conducted in porous media consisting of glass beads or silica sand. The glass beads and silica sand were treated with an organosilane to alter the wettability in the oil-wet experiments. A laboratory setup incorporating the LabView data acquisition system was used to record the oil production in the gas displacement experiments. The ultimate oil recovery was important in deciding the effect of wettability and fractures on the GAGD performance.

Two series of gas displacement experiments were conducted using n-decane. The first series utilized both water-wet and oil-wet porous media to investigate whether the wettability of the porous medium affected the GAGD recovery at all. Within the first series of experiments, the mode of gas injection (i.e. secondary mode or tertiary mode), the strategy of gas injection (meaning a constant pressure gas displacement or a constant rate displacement), and the type of gas injected was varied to assess the effect of the variation of these parameters on the GAGD performance. Depending on the intended range of the Bond number, the grain size diameter of the porous medium was varied by using either glass beads or silica sand in the physical model. The subsequent series of experiments was aimed to study the effects of the presence of a fracture in the porous medium on the oil recovery. These experiments utilized a custom-made fracture simulation, the use of n-decane, and both water-wet and oil-wet porous media to study the complete gamut of effects on the GAGD oil recovery.

Thus, the significant contribution of this study will be the experimental proof of the effect of the wettability of the porous medium and the presence of a fracture on improving the performance of GAGD process.

## **CHAPTER 2**

### **LITERATURE REVIEW**

The focus of this study is the effect of wettability and fractures on the improvement of the GAGD performance. As such, the literature review emphasizes the various factors pertaining to oil recovery through gravity drainage, specifically the GAGD process, and the simulation of fractures within gas displacement experimental work.

#### **2.1 Enhanced Oil Recovery (EOR) Methods**

##### **2.1.1 Introduction**

Traditional primary and secondary oil recovery methods typically recover one-third of the original oil in place, leaving the rest behind. During the life of a well there is always a point at which the cost of producing an additional barrel of oil is higher than the market price. Under normal circumstances, the well is abandoned at that point. According to Lake (1989), enhanced oil recovery (EOR) is oil recovery by the injection of materials not normally present in the reservoir. This definition embraces all modes of oil recovery processes and covers many oil recovery agents. It also does not restrict EOR to a particular phase in the producing life of a reservoir, be it primary, secondary, or tertiary. Primary recovery is oil recovery by natural drive mechanisms, such as solution gas, water influx, gas cap drive, and gravity drainage. Secondary recovery refers to techniques such as gas or water injection, which maintain the reservoir pressure. Tertiary recovery is any technique applied after secondary recovery. This definition of EOR does, however, exclude waterflooding and methods involving the injection of gases already present in the reservoir. An overview of the various oil recovery mechanisms is presented in Figure 2.1. There has been a renewed interest in applying EOR methods because the aging oil fields in the US and Canada are declining faster than new oil is being added by discoveries. Given the declining reserves and the low probability of locating significant new fields, producers have sought ways of producing any additional oil in existing fields, making North America a proving ground for EOR techniques (refer to Table 2.1).

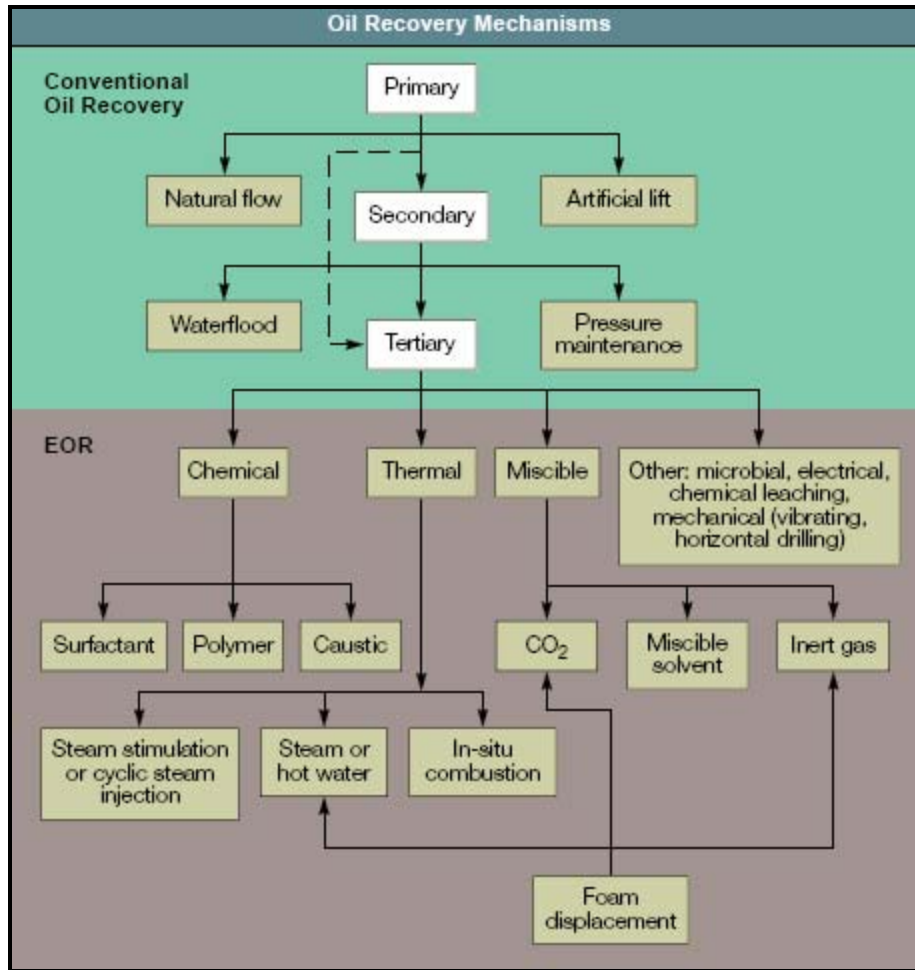


**Figure 2.1:** Overview of Oil Recovery Mechanisms (Lake, 1992)

**Table 2.1:** Estimated Annual Worldwide Production of Oil by EOR circa January 1992 (Lake, 1992)

Estimated Annual Worldwide EOR Produced Oil, B/D (x1000)					
Country	Thermal	Miscible	Chemical	EOR Total	%
USA	454	191	11.9	656.9	42
Canada	8	127	17.2	152.2	10
Europe	14	3	—	17.0	1
Venezuela	108	11	—	119.0	7
Other S. American	2	NA	NA	17.0	1
USSR	20	90	50.0	160.0	10
Other (estimated)	171*	280**	1.5	452.5	29
Total	777	702	80.6	1574.6	100

### 2.1.2 Types of EOR

Most EOR methods fall distinctly into one of three categories:

1. Thermal methods (application of heat) – thermal methods are the main methods to recover heavy oils (with a density lower than 20 °API and a viscosity between 200 and 10,000 centipoises) and bitumen (with a viscosity ranging from 10,000 to 1,000,000 centipoises). Such heavy oils do not respond well to primary production or waterflooding, so the initial oil saturation is typically high at the start of a thermal recovery project. The principle of thermal methods is to increase the oil's temperature thereby reducing the viscosity. The two primary methods of heating reservoir oil are the injection of fluid heated at the surface and the production of heat directly within the reservoir by burning some oil in place.
2. Chemical methods (flooding with chemicals) – chemicals used in EOR are polymers, surfactants, and alkalis. All are mixed with water and other chemicals before injection. Targets for chemical recovery are crude oils in the range between the heavy oils recovered by thermal processes and the light oils (with a density of at least 22° API and a viscosity less than 100 centipoises) recovered by miscible gas injection.
3. Miscible methods (mixing of oil with a solvent) – represents the fastest growing sector within EOR development. Miscible floods use a solvent that mixes fully with the residual oil to overcome capillary forces and increase oil mobility. The displacement efficiency nears 100% where the solvent contacts the oil and miscibility occurs. The numerous successful solvents include liquefied petroleum gas, nitrogen (N<sub>2</sub>), carbon dioxide (CO<sub>2</sub>), flue gas (mainly nitrogen and CO<sub>2</sub>), and alcohol. Miscible displacement EOR can be subdivided into three significant processes: miscible slug, enriched gas, and high-pressure lean gas (including CO<sub>2</sub>). Early breakthrough of the solvent and viscous fingering resulting in the bypassing of substantial amounts of oil have plagued many field implementations of miscible flooding.

It is the opinion of Lake (1992) that the major contribution to EOR will most likely come from constantly improving the art of reservoir characterization for predicting EOR response and from horizontal drilling.

## **2.2 The Development of the Gas-Assisted Gravity Drainage (GAGD) Process**

### **2.2.1 Introduction**

It has been stated by Rao et al. (2004) that within the period of 1990 to 2002 the number of miscible CO<sub>2</sub>-injection projects has increased from 52 to 66. Their study indicates that while the number of CO<sub>2</sub> miscible projects has steadily increased over the last two decades, all other gas injection projects have declined except for the hydrocarbon miscible projects. Overall, the share of production from gas injection enhanced oil recovery in the United States has almost doubled from 23% in 1990 to 44.5% in 2002. This demonstrates the growing commercial interest that the oil industry has had in gas injection projects. The relatively high price of natural gas has only fanned this growing interest.

The accepted practice in industry is the implementation of the Water Alternate Gas (WAG) process. First proposed by Caudle and Dye in 1958, it still remains the default option for mobility control in horizontal gas floods. Mobility control is one of the biggest factors controlling the success of a gas injection project because the viscosity of the injected gases generally is less than one-tenth of that of the oil at reservoir conditions. Christensen et al. (1998) have concluded that in a majority of the 59 projects as reviewed by them, the incremental oil recovery was in the range of 5% to 10%, with an average incremental oil recovery of 9.7% for miscible WAG projects and 6.4% for immiscible WAG projects. In comparison, the oil recoveries were much better (in the range of 15% to 44% of the original oil in place) in the gravity-stable vertical gas floods conducted in pinnacle reefs of Alberta. These field results indicate the benefit of working with nature by making use of the buoyancy rise of the injected gas to displace oil downwards.

### **2.2.2 The Concept behind the GAGD Process**

The idea behind the development of the GAGD process occurred to Rao et al. (2004) as a natural extension of the gravity-stable gas injection process in Alberta, which demonstrated that working with nature yields significant benefits (oil recoveries in the range of 15 % to 40%OOIP) over processes designed to combat the natural phenomenon of gravity segregation. The concept of the GAGD process is gas injected in vertical wells accumulates at the top of the payzone due to gravity segregation and displaces oil, which

drains to the horizontal producer straddling several injection wells near the bottom of the payzone (see Figure 2.2). As injection continues, the gas chamber grows downwards and sideward resulting in larger and larger portions of the reservoir being swept by it without any increase in the water saturation in the reservoir, thus maximizing the volumetric sweep efficiency. The gravity segregation of the injected gas also helps in delaying the gas breakthrough to the producer as well as preventing the gas phase from competing for flow with the oil. The process makes use of any existing vertical wells in the field for gas injection and calls for drilling a long horizontal well for the production of the draining oil (Rao et al., 2004).

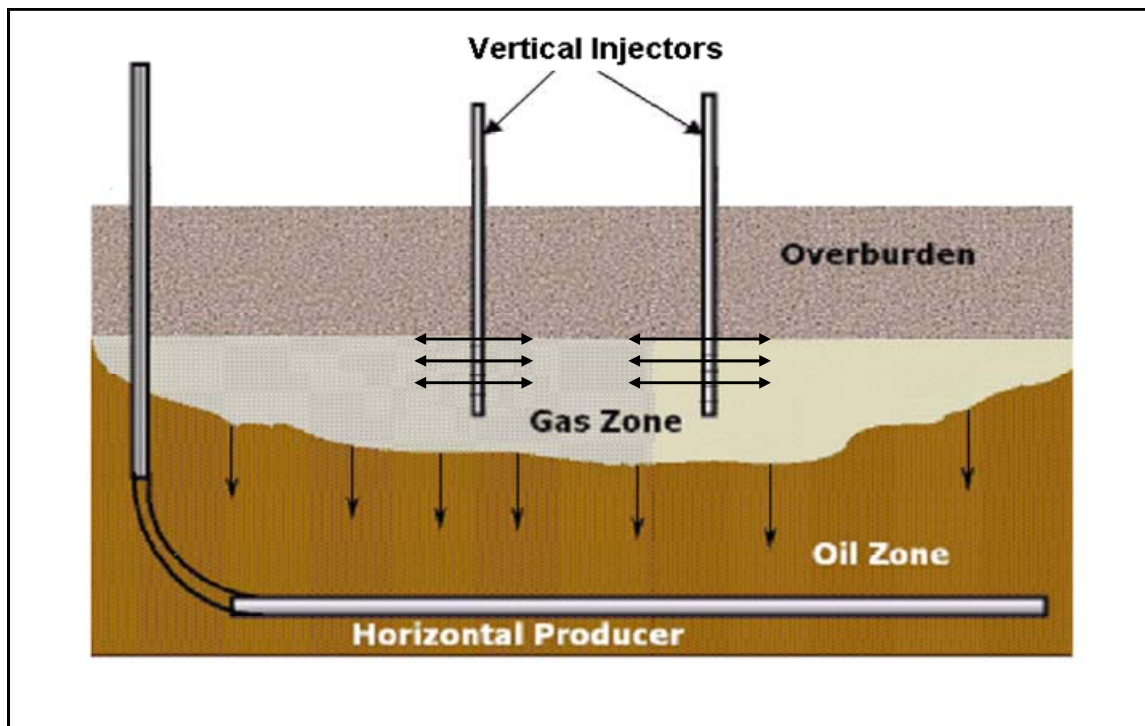


**Figure 2.2:** The Concept behind the GAGD Process (Rao et al., 2004)

### 2.2.3 Developments in Horizontal Drilling

Biglarbigi et al. (2000) state that the Department of Energy National / Petroleum Technology Office (DOE/NPTO) has developed a comprehensive data system for the evaluation of the potential of horizontal wells in the lower 48 states. In their assessment study they state that since 1984, this system has been maintained and operated as a planning and analysis tool to address important policy issues regarding research and

development, economic incentives, and environmental regulations. In 1997, the DOE/NPTO worked very closely with industry representatives to identify the target resource for horizontal well technology and evaluate its future recovery potential.

Since 1990, the pace of drilling has kept up a fairly constant pace of about 600 to 1,000 wells/year, with the main use for the horizontal wells as part of development of naturally fractured reservoirs, particularly in the prolific Austin chalk. These reservoirs often consist of so-called compartments that are long and parallel or sub-parallel to natural vertical fractures from which oil and gas can be produced. Horizontal wells can be drilled several thousand feet laterally through the formation to connect multiple fractures or compartments to the wellbore, thereby improving the chance for commercial production of oil and gas. Horizontal wells also have the characteristic to produce at relatively high rates with low pressure differential between the reservoir and the wellbore. These factors, along with favorable geometry, make horizontal wells very attractive for application in reservoirs with water and gas coning problems. That is why approximately one-third of the horizontal wells in the U.S. have been drilled to minimize coning. With the continued and steady development of horizontal drilling technology and development of improved diagnostic tools horizontal wells will also be applicable to the areas of injection-profile modification, thin-bed reservoirs, and continuity improvement (Biglarbigi et al., 2000).

With current oil prices the potential reserves with horizontal wells could be over a billion barrels. This clearly provides a unique opportunity for a focused effort to promote application of the technology nationwide.

## **2.3 The Effect of Wettability on Oil Recovery**

### **2.3.1 Introduction**

Wettability is the term used to describe the relative adhesion of two fluids to a solid surface (Tiab et al., 1996). In a porous medium containing two or more immiscible fluids, wettability is a measure of the preferential tendency of one of the fluids to adhere to the surface. According to Morrow (1990), the reservoir wettability is determined by complex interface boundary conditions acting within the pore space of sedimentary rocks. These conditions have a dominant effect on interface movement and associated oil

displacement. Wettability is a significant issue in multiphase flow problems ranging from oil migration from source rocks to enhanced oil recovery methods such as alternate injection of CO<sub>2</sub> and water. Reservoir wettability is not a simply defined property and classification of reservoirs as just water-wet or oil-wet is a gross simplification.

In a water-wet brine-oil-rock system, water will occupy the smaller pores and wet the majority of the surfaces in the larger pores. In areas of high oil saturation, the oil rests on a film of water spread over the rock surface. If the rock surface is preferentially water-wet and the rock is saturated with oil, water will naturally imbibe into the smaller pores, displacing oil from the core.

However, if the rock surface is preferentially oil-wet and the core is saturated with water, it will naturally imbibe oil into the smaller pores, displacing water from the core. Thus, a core saturated with oil is water-wet if it imbibes water spontaneously and, conversely, a core saturated with water is oil-wet if it imbibes oil spontaneously. The wettability of a reservoir can range from strongly water-wet to strongly oil-wet depending on the brine-oil interactions with the rock surface.

Some descriptive terms that are applicable to describe the wettability of a brine-oil-rock system are:

1. Neutral or intermediate wettability – this occurs when the rock displays no preference for either oil or water; the system can be equally wetted by both oil and water.
2. Fractional wettability – implies a spotted, heterogeneous wetting of the surface. Fractional wettability means that scattered areas throughout the rock have different degrees of wettability (either water-wet or oil-wet). Fractional wettability occurs when the surfaces of the rock are composed of various minerals that have very different surface chemical properties, leading to variations in wettability throughout the internal surface of the rock. Fractional wettability should not be confused with a state of neutral wettability, meaning that the rock surfaces have an equal affinity to oil and water. Cores exhibiting fractional wettability will imbibe a small quantity of water when the oil saturation is high, and also will imbibe a small amount of oil when the water saturation is high.
3. Mixed wettability – this term is commonly used to refer to the condition where the smaller pores are occupied by water and are water-wet, whereas the larger pores of

the rock are oil-wet, and a continuous filament of oil exists throughout the core in the larger pores. Because the oil is located in the larger pores of the system in a continuous path, oil displacement from the rock occurs even at very low oil saturation. That is why the residual oil saturation of mixed-wettability rocks is unusually low. Mixed wettability can occur as a result of the invasion of oil containing interfacially active polar organic compounds into a water-wet rock saturated with brine. After having displaced the brine from the larger pores, the interfacially active compounds react with the rock's surface, displacing the remaining aqueous film and producing an oil-wet lining on the surface within the larger pores. The water film between the rock and the oil in the pore is stabilized by a double layer of electrostatic forces. As the thickness of the film is diminished by the invading oil, the electrostatic force balance is destroyed and the film ruptures, allowing the polar organic compounds in the oil to react directly with the rock surface (Tiab et al., 1996).

The silicate-water interface is acidic and, therefore, only the basic constituents in crude oils (generally nitrogen-containing compounds) will readily adsorb to the surface rendering it oil-wet. In contrast, the carbonate-water interface is basic and the acidic compounds in crude oils (those containing carboxylic and phenolic groups) will readily adsorb onto the surface. Even though crude oils generally contain acidic polar compounds, the silicate rocks tend to be neutral to water-wet and the carbonate reservoir rocks tend to be neutral to oil-wet.

Several methods have been used to alter the wettability of reservoir rocks:

1. Treatment with organosilanes (general formula  $(\text{CH}_3)_n\text{SiCl}_x$ ), which causes the silanes to chemisorb on the silica surface producing hydrochloric acid and exposing the methyl groups, thus producing the oil wetting characteristics.
2. Aging under pressure in crude oils.
3. Treatment with naphthenic acid.
4. Treatment with asphaltenes.
5. Addition of surfactants to the fluids.

Many more techniques are currently employed by different researchers.

### 2.3.2 Spreading

Together with the wettability, the spreading characteristics of a system are key factors in three-phase gas injection (Vizika et al., 1994). Spreading comes into play when connate water is considered and the effect of oil film flow due to the spreading of oil on water in the presence of gas is considered.

The spreading coefficient of oil on water in the presence of gas,  $S_o$ , is defined as a balance of interfacial tensions:

$$S_o = \sigma_{wg} - (\sigma_{wo} + \sigma_{og}) \text{-----} (1)$$

where:

- $\sigma_{wg}$  is the interfacial tension between water and gas;
- $\sigma_{wo}$  is the interfacial tension between water and oil;
- $\sigma_{og}$  is the interfacial tension between oil and gas.

**Water-wet media:** When  $S_o$  is positive, the oil tends to form spreading films on the water substrate in presence of gas, thus favoring the hydraulic conductivity of the oleic phase. This leads to very low residual oil saturation due to the fact that oil remains continuous through the spreading films. In case  $S_o < 0$ , the absence or rupture of oil spreading films leads to early disconnection of the oil into pockets that remain trapped due to lack of continuity. However, this phenomenon is only important when film flow is dominant. During the period of bulk drainage, no significant difference is noticed (Vizika et al., 1994).

**Oil-wet media:** For both spreading and non-spreading conditions, the hydraulic conductivity of the oil is assured by the oil wetting films on the surface. Here, the spreading coefficient of oil on water plays a minor role. The oil always remains continuous and locally low oil saturations may be obtained, but the overall displacement efficiency deteriorates due to strong surface forces causing adhesion.

### 2.3.3 Fluid Displacement Energy

When a core is strongly water-wet the core will imbibe water until the water saturation equals the water saturation at the residual oil saturation. This means that the work

required for oil displacement is almost zero for a strongly water-wet system. The amount and rate of imbibition depend on a number of simultaneously acting properties of a water-wet system: the wettability of the system, the interfacial tension, the saturation history of the system, the initial saturation, the fluid viscosities, the pore geometry, and the pore size distribution.

As the system becomes less water-wet, the work required for displacement of oil increases and the amount and rate of imbibition decrease. This means that a smaller amount of water will imbibe at a lower rate as the system becomes less water-wet.

If the system is oil-wet, oil will spontaneously imbibe into the system displacing the water. Water must be forced into the system and the work required for the displacement of oil by water is, in theory, the work required for a waterflood, an economic factor of oil production.

#### **2.3.4 Wettability and Oil Recovery – Waterfloods**

Primary oil recovery is affected by the wettability of the system because a water-wet system will exhibit greater primary oil recovery, but the relationship between primary recovery and wettability has not been developed (Tiab et al., 1996). Most of the studies on the effects of wettability on oil recovery have been focused on waterflooding and the analyses of the behavior of relative permeability curves. In laboratory displacement tests designed to investigate the effects of wettability on oil recovery, early results showed a decrease of the oil recovery with decreasing water-wetness of the cores (Morrow, 1990). This is consistent with the intuitive notion that strong wetting preference of the rock for water and associated strong capillary imbibition forces give the most efficient oil displacement. However, there are an increasing number of examples of improved recovery with a shift from strongly water-wet conditions being reported for weakly water-wet to intermediate wetting conditions (these results generally involve displacement of crude oils or refined oils from cores in which organic films have been deposited from crude oil). When the wettability is varied from water-wet to oil-wet, the recovery is seen to pass through a maximum when the wettability is close to neutral. Results showed that a shift towards less water-wet conditions can range from highly adverse to being highly beneficial to oil recovery (Morrow, 1990). Experiments conducted by Morrow (1990) to evaluate the effect of wettability on residual oil

saturation show that the residual oil saturation is least for systems at neutral wettability and increases as the system becomes more water-wet or oil-wet. A strongly water-wet core will produce most of the oil before water breakthrough and the water/oil ratio will increase rapidly thereafter, thus diminishing production to an insignificant amount. An oil-wet core will produce water early at a low water/oil ratio, which will continue to increase gradually.

Departure from very strongly water-wet conditions can give distinctly reduced oil entrapment. In 2-D pore network flow experiments (Li and Wardlaw, 1986) that permit observation of pore-level displacement mechanisms affecting displacement efficiency, it has been noted that residual oil is trapped as disconnected globules in the pore bodies of systems that were very strongly water-wet and had a high aspect ratio (i.e., high ratio of pore body to pore size) believed to be typical of reservoir rocks. Simulated waterfloods of crude oil from micromodels were also conducted at various wettability conditions by Li and Wardlaw (1986), and while a great variety of distributions has been observed, no crude-oil/brine system showed the extensive trapping of oil in the pore bodies that is characteristic of very strongly water-wet systems. Li and Wardlaw (1986) also showed that snap-off in simple pore models of rectangular cross sections can be inhibited if the water-advancing contact angle exceeds 60°.

### **2.3.5 Wettability and Oil Recovery – Gas Injection**

The efficiency in recovering a large fraction of the waterflood residual oil from water-wet porous media by low pressure inert gas injection assisted by gravity drainage has been reported by Naylor & Frørup (1989). They conducted a series of experiments to investigate secondary and tertiary, gravity-stable, immiscible, nitrogen displacement of oil. Two high pressure and four low pressure experiments were performed using cores that consisted of well-cemented aeolian sandstone, which was water-wet, had well sorted grains and a low clay content. The high pressure runs were conducted to investigate the effects of core orientation during gas injection. Secondary injection was conducted in the presence of a connate water saturation, and tertiary injection was conducted following a waterflood. The results from the study demonstrated that the oil production can be enhanced when gravity forces assist the drainage of oil during gas displacement, and, furthermore, that a decrease in initial water saturation resulted in an increase of oil

permeability during gas injection. In general, the authors concluded that improvement in oil recovery may be achieved by secondary or tertiary gravity-stable gas injection, even in the absence of favorable compositional and/or interfacial tension effects.

Catalan et al. (1994) reported experimental results obtained with oil-wet consolidated media. It was their goal to study tertiary gravity drainage in cores of varying wettability. They conducted experiments with water-wet and oil-wet Berea, oil-wet Pembina Cardium cores, and glass bead packs. The Berea core was made oil-wet by treatment with a 4% solution of dichlorodimethylsilane (drifilm) in hexane. They found that the displacement mechanisms of oil during tertiary gravity drainage are different in water-wet and oil-wet porous media. In water-wet media, the spreading of oil as a film between the gas occupying the center part of the pores and the aqueous phase covering the pore walls is essential to establish and maintain continuity of the oleic phase. By contrast, when the oil is the wetting phase, spreading is not important because the waterflood residual oil phase is always present as a continuous film on the pore walls. Some of the conclusions of this study are:

1. Tertiary gravity drainage in water-wet systems is most efficient when the oil can spread on water in the presence of gas (i.e. positive spreading coefficient of oil).
2. Tertiary gravity drainage promises to be a very effective enhanced oil recovery method in oil-wet reservoirs.
3. Microscopic, pore-scale heterogeneities decrease the recovery efficiency.

Flow visualization experiments using macroscopically homogeneous glass micromodels helped show the role played by pore-level heterogeneities. In a random network of pore bodies connected by large pore throats imbedded in a network of smaller pore throats and pore bodies, it was observed that several segments of bypassed oil (waterflood residual oil) were successfully drained during gravity drainage. With the gas oil contact maintained constant, further drainage of oil, further reconnection of isolated residual oil, and further redistribution of residual oil took place, but, in all, residual oil recovery by gravity drainage from bypassed regions was found to be a very slow process.

Ren et al. (2004) conducted a pore-level observational study of gas-assisted tertiary gas-injection processes to achieve a better understanding of the pore-level mechanisms. They used a transparent 3-D sandpack model and conducted updip waterflooding and tertiary

gas injection to observe how the fluids flowed and to observe how the mobilization of the residual oil in a single pore took place after gas invasion or water invasion occurred. Of greatest interest to them was to see whether oil films and oil film flow occurred and to understand the mechanism underlying fluid flow in a single pore space. Some of their observations were as follows:

After the waterflood, the residual oil was distributed sparsely as isolated oil globules. There was very little bypassed oil owing to the relatively low degree of heterogeneity of the porous medium within the cell. When gas injection was started in the cell, it was observed that the gas front was not as flat as that of the oilflood and the waterflood. The gas front in the cell undulated significantly. Gas had a tendency to go faster in the middle of the cell first, then the front extended to both sides of the cell. However, it was observed that undulations of the front were always at the same level until they reached the outlet.

The fingering occurred mainly because of the very low viscosity of the gas and the small size of the cell.

Under the microscope, the oil in these spots was in continuous form. As the gas front moved downward, brown spots were joined by more residual oil, and the spots became linked together. Therefore, an oil bank was formed. When the oil bank moved out of the outlet, most of the residual oil was produced.

When gas was entering pores that contained water and oil, it darted quickly into these pores and occupied most of the pore space. Then, the gas stayed still for quite a while before it darted forward again. As the gas entered a pore, some oil was displaced out of the pore. It was observed that some of the oil flowed out immediately before the invasion of gas. Some oil was left, so an oil layer or oil film was observed at the edge of the gas, or between the water and the gas. The residual oil and these oil films and oil layers were all linked together. Thus, the continuity of the oil was formed; this continuity provided a way for the oil to flow downward under its own weight. As time went on, gas entered all the pores, and, furthermore, gas occupied all of the available space in these pores. On the basis of this observation, it is thought that the oil flowing through the oil films is driven not only by its own weight but also by the increasing volume of the gas. When gas enters a pore, the pressure of the gas must be higher than the threshold capillary pressure of the pore. This pressure is much higher than the oil or water pressure in the pore so that the gas moves quickly when it enters a pore. As the gas pressure builds up again before entering other pores, this pressure will also force more gas into a preoccupied pore and push the oil and water out of the pore. Once gas breakthrough occurs, however, the effect of the increased gas volume will be very small. (pp. 196-197)

## **2.4 Determination of the Wettability**

There are many different ways for measuring the wettability of a system. They include quantitative methods, such as contact angle measurement, imbibition/forced displacement

(the Amott method), the United States Bureau of Mines (USBM) wettability method, and qualitative methods, such as imbibition rates, microscope examination, flotation, glass slide method, relative permeability curves, and more. Although no single method is accepted by everyone, three quantitative methods are generally used:

1. Contact angle measurement.
2. The Amott method.
3. The USBM method.

The contact angle is a measure of the wettability of a specific surface, while the Amott and the USBM method measure the average wettability of a core.

### 2.4.1 The Contact Angle

When two immiscible fluids are in contact the fluids are separated by a well-defined interface, which is only a few molecular diameters thick. When the interface is in intimate contact with a solid surface it intersects the surface at an angle, the contact angle,  $\theta$ , which is a function of the relative adhesive tension of the liquids to the solid. The angle is described by Young's equation:

$$\cos\theta = \frac{(\sigma_{s1} - \sigma_{s2})}{\sigma_{12}} \text{-----} (2)$$

where:

- $\sigma_{s1}$  = interfacial tension between the solid and fluid 1;
- $\sigma_{s2}$  = interfacial tension between the solid and fluid 2;
- $\sigma_{12}$  = interfacial tension between the two fluids.

The contact angle is the best wettability measurement method when pure fluids and artificial cores are used because there is no chance of surfactants or other compounds altering the wettability (Anderson, 1986). Some of the methods used to measure the contact angle include: the tilting plate method, sessile drop or bubbles, vertical rod method, tensiometric method, cylinder method, capillary rise method, and the Dual Drop Dual Crystal method.

### 2.4.2 The Amott Method

The Amott method combines imbibition and forced displacement to measure the average wettability of a core. In this method both reservoir core and fluids can be used. The Amott method is based on the principle that the wetting fluid will generally imbibe spontaneously into the core, displacing the non-wetting one. The ratio of spontaneous imbibition to forced displacement is used to reduce the influence of other factors, such as relative permeability, viscosity, and the initial saturation of the rock.

Usually the core is prepared by centrifuging under brine until the residual oil saturation is reached. The following four steps are then executed in the Amott method:

1. Immerse the core in oil and measure the volume of water displaced by the spontaneous imbibition of oil after 20 hours.
2. Centrifuge the core in oil until the irreducible water saturation is reached and measure the total amount of water displaced, including the volume displaced by spontaneous imbibition.
3. Immerse the core in brine and measure the volume of oil spontaneously displaced by the imbibition of water after 20 hours.
4. Centrifuge the core in brine until the residual oil saturation is reached and measure the total amount of oil displaced.

Note that the core may be driven to the irreducible water saturation and the residual oil saturation by flow rather than using a centrifuge. This is especially necessary for unconsolidated material that cannot be centrifuged.

The test results are generally expressed as follows:

1. The displacement-by-oil ratio:

The ratio of the water displaced by spontaneous oil imbibition alone,  $V_{wsp}$ , to the total volume of water displaced by oil imbibition and forced displacement,  $V_{wt}$ .

$$\delta_o = \frac{V_{wsp}}{V_{wt}} \text{-----} (3a)$$

2. The displacement-by-water ratio:

The ratio of the oil volume displaced by spontaneous imbibition of water,  $V_{osp}$ , to the total oil volume displaced by imbibition and forced displacement,  $V_{ot}$ .

$$\delta_w = \frac{V_{osp}}{V_{ot}} \text{-----} \quad (3b)$$

Preferentially water-wet cores have a positive displacement-by-water ratio and a zero value for the displacement-by-oil ratio. The displacement-by-water ratio approaches one as the water-wetness increases. Similarly, oil-wet cores have a positive displacement-by-oil ratio and a zero displacement-by-water ratio. Both ratios are zero for neutrally wet cores. The time period for the spontaneous oil and water imbibition steps were chosen arbitrarily, but it is recommended that the cores be allowed to imbibe until either imbibition is complete or a pre-set maximum time limit has been reached. Imbibition can take from several hours to more than two months to complete.

## **2.5 The Alteration of the Wettability of the Glass Beads through Silylation**

### **2.5.1 Introduction**

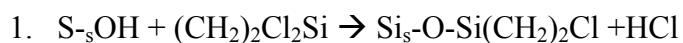
Silylation is the chemical reaction in which an active hydrogen atom (usually in a hydroxyl group) is displaced by an organosilyl group. Surfaces are silylated to impart hydrophobicity or an organic nature to inorganic surfaces. Alkylsilylating agents convert surfaces to water-repellent, low-energy surfaces useful in water-resistant treatments (Plueddemann, 1982). Methylchlorosilanes react with water or hydroxyl groups at the surface to liberate hydrochloric acid (HCl) and deposit a very thin film of methylpolysiloxanes that has a very low critical surface tension and is, therefore, not wetted by water (Plueddemann, 1986).

### **2.5.2 The Silylation Reaction Mechanism**

Organosilanes possess two classes of functionalities and have the general formula  $R_nSiX_{(4-n)}$ . Bonding to the substrate occurs through the hydrolyzable group (X), typically a halogen, alkoxy, acyloxy or amine. While halo and aminosilanes can be reacted directly with a silica substrate, the usual procedure is to hydrolyze the silane prior to reaction with the surface. It is the non-hydrolyzable R-group which imparts the desired characteristics to the modified surface. As the symbol R implies, the non-hydrolyzable group usually consists of an alkyl chain that can contain a myriad of functional groups, reflecting the very diverse fields in which modified surfaces are employed.

Water required for the hydrolysis of the organosilanes can be provided by the silica substrate, the atmosphere or generated in-situ. In traditional methods aqueous solutions are employed. The silanol moieties (SiOH) resulting from the hydrolysis of the X-group are usually quite labile and readily condense to form siloxane (Si-O-Si) bonds with other silanols, either on the siliceous surface or in the solution. Typically, the hydrolyzed silanes condense in the aqueous solution, forming siloxane-linked oligomers. These siloxane oligomers interact with the substrate by hydrogen-bonding to the surface silanols. In practice, it is difficult to precisely control the extent of oligomerization, resulting in nonreproducible surface coverage. Covalent bonds with the surface are formed via condensation with the surface silanols during a drying or curing step. The curing process, the substrate properties and the solution species that interact with the surface all play a role in determining the characteristics of the modified surface. Frequently, when a silane with three hydrolyzable groups is employed, extensive crosslinking occurs, which produces a three-dimensional silane multilayer on the surface rather than a two-dimensional monolayer. Reacting the silica substrate with organosilanes possessing only one hydrolyzable group can produce monolayer coverages. However, the resultant surfaces will still exhibit some silica characteristics because of unreacted silanol groups and are not as hydrolytically stable as the crosslinked surfaces. The need for a modified surface possessing the stability produced by crosslinking, yet retaining the reproducibility and the properties of a true monolayer has led to the development of silylation techniques from organic solvents. When an organosilane in a dry organic solvent solution contacts a silica substrate, a rapid physisorption of unhydrolyzed silane occurs. The extent of this adsorption is primarily determined by the nonhydrolyzable silane functionality. Once adsorbed, the silane is hydrolyzed by surface water. Secondary adsorption of the silane onto the modified surface occurs during the hydrolysis process (Morrall, 1986).

The interaction of certain silane compounds, in particular the chlorosilanes, with silica surfaces has important utility in their use as surface deactivating agents. When considering the reaction of dimethyldichlorosilane, or DMDCS ((CH<sub>2</sub>)<sub>2</sub>Cl<sub>2</sub>Si), with the silica surface, two possible reactions can be presumed:





A mixed, 1.6 order reaction has been observed suggesting that both reactions do occur. This implies that 40% of the freely vibrating surface hydroxyl groups reacts monofunctionally, but 60% must be present in a position sufficiently close to each other that they can react in a bifunctional manner. It is not possible to tell from either spectroscopic or kinetic data whether these are geminal or vicinal groups on the surface, only that they are not hydrogen-bonded to each other (Hair, 1986).

The initial condensation of alkoxysilanes with mineral surfaces may be driven to completion by heating and adding a catalyst for the condensation. A drying temperature of 120 °C – 200 °C may be required to ensure sufficient bonding of alkoxysilanes with silica. Amines, titanate esters and tin compounds are catalysts for the condensation of alkoxysilanes with mineral surfaces. Neutral alkoxysilanes are best bonded in the presence of an organic amine or of an amino-organofunctional silane (Hair, 1986).

## **2.6 Fracture Simulation within the GAGD Process**

### **2.6.1 Literature Review**

Darvish et al. (n.d.) conducted a numerical study in order to design oil-CO<sub>2</sub> gravity drainage laboratory experiments of a naturally fractured reservoir. They conducted the study using a fully compositional simulation model to investigate the drainage of CO<sub>2</sub> from a chalk core with artificial fractures. They also included the effects of molecular diffusion and interfacial tension. In their experiments, they used a cylindrical chalk core as the porous medium with a concentric hole through the middle of the core acting as an artificial fracture.

The numerical results examined the effects of core geometry, matrix permeability, pressure, and gas type in the fracture system on the oil recovery under CO<sub>2</sub>/oil gravity drainage. Some of the most interesting results from their study can be summarized as follows:

1. The oil recovery scales up as the matrix permeability increases.
2. Increasing pressure postpones the oil recovery. The density difference reduces as the pressure increases and, consequently, this reduces the gravity force and results in less recovery at the early stage. The ultimate recovery for a high-pressure case is higher

than for a low-pressure case, which is caused by the high extraction capability of CO<sub>2</sub> at high pressure.

3. The recovery performance for the injection of hydrocarbon gas versus CO<sub>2</sub> into the matrix is always higher at all stages due to the low hydrocarbon gas density compared with the CO<sub>2</sub> density.
4. In the case of CO<sub>2</sub> injection the recovery mechanism can be divided into two stages: (i) diffusion and gravity drainage and (ii) the extraction mechanism. In the initial stage, transport of the injection gas from the fracture into the matrix occurs primarily by lateral liquid-liquid diffusion between the undersaturated oil inside the matrix and the saturated oil with CO<sub>2</sub> at the inner surface of the matrix while at the same time the gas enters from the top of the block due to gravity drainage. This can be seen from the viscosity reduction of the oil along the core in the diffusion case. The CO<sub>2</sub> diffusion into the core causes the oil to swell followed by viscosity reduction and, consequently, less viscous forces and higher drainage rates. In the extraction mechanism, most heavy components of the residual oil are vaporized into the gas phase.

### **2.6.2 Fracture Simulation**

In addition to the secondary and tertiary water-wet and oil-wet runs, gas displacement runs were conducted in which the presence of a fracture was simulated. This was done by placing a mesh box inside the physical model prior to filling it up with glass beads. The mesh box consisted of strip metal wrapped in such a way as to form a framework with the length of the inside of the physical model and a height equal to the width of the model (dimensions: 13 7/8" by 1" by 1/2"). The framework was covered with 400-mesh sieve cloth to keep open an internal space that spanned the entire inner height of the model (the fracture) and, at the same time, to allow flow through it (see Figure 2.3).

## **2.7 Scaling Groups for Experimental Set-up**

### **2.7.1 Introduction**

According to Grattoni et al. (2001) gas injection is an attractive three-phase oil recovery method where capillary, buoyancy, and viscous forces control fluid displacement and flow within a porous medium. Gravity causes segregation of the fluids according to their

density, but fluid viscosity, interfacial tensions, wettability and pore geometry affect the rate. When the vertical permeability of the reservoir is high, the effect of gravity can become dominant. The capillary pressure is the combined effect of interfacial tensions and the rock characteristics (pore geometry and wettability) and controls the equilibrium configuration of the fluids. Any change in these interactions can modify the trapping and movement of gas-oil-water.

Three-phase flow is governed by the pore-scale effects, and the displacement mechanisms are controlled by the fluid morphology as well as by the viscosity, wettability, spreading coefficients, and pore geometry. In oil-wet conditions the oil forms a wetting film on the solid and the non-wetting fluids occupy the larger regions of the pore space, so that water can block gas advance and restrict oil movement. The fluid configurations can create conditions that create different gravity drainage recoveries due to changes in the morphology of the fluids and the balance of gravity, viscous, and capillary forces.

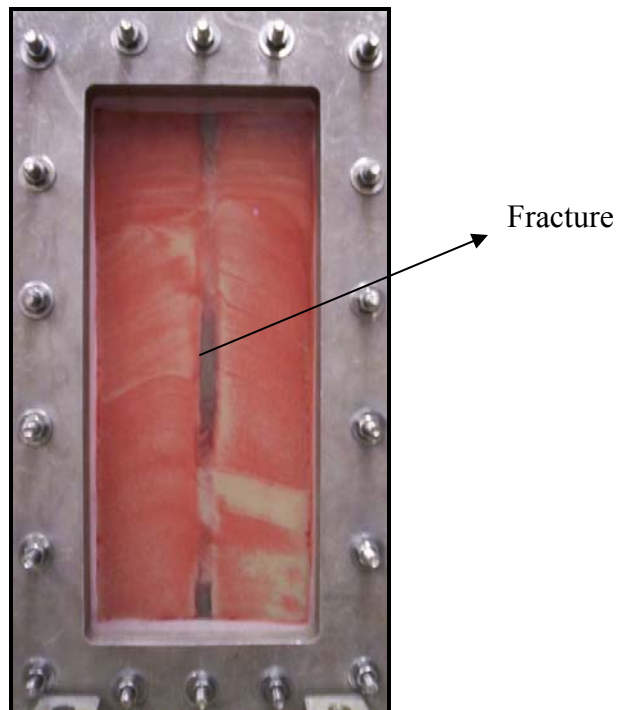


**Figure 2.3:** Physical Model with Vertical Fracture Simulation

### 2.7.2 Dimensionless Groups

The ratios between the different forces can be expressed through dimensionless groups and can be used to understand the influence of different forces during gravity drainage processes (Grattoni et al., 2001).

The balance between the viscous and the capillary forces during gravity dominated flow can be described by the capillary number  $N_C$ . The capillary number measures the relative strength of the viscous to the capillary forces. It can be defined as:

$$N_C = \frac{v \mu}{\sigma \cos\theta} \text{-----} (4)$$

where:

- $v$  is the Darcy velocity;
- $\mu$  is the viscosity of the displacing phase;
- $\sigma$  is the interfacial tension.
- $\theta$  is the contact angle.

Variations in the pore size distribution or the degree of consolidation produce changes in the value of the capillary number due to the change in trapped oil distribution.

The Bond number,  $N_B$ , is a dimensionless group that measures the relative strength of gravity and capillary forces. For the trapping of the non-wetting phase, it can be expressed as:

$$N_B = \frac{\Delta\rho g l^2}{\sigma} \text{-----} (5)$$

where:

- $\Delta\rho$  is the density difference between the two fluids;
- $g$  is the gravitational constant;
- $l$  is a characteristic length of the porous medium.

The Bond number can also be written to include the relative magnitude of the viscous, buoyancy, and capillary forces within the pore structure that control the movement of the interfaces:

$$N_B = \frac{\Delta\rho_{og} g Z R_a}{2\sigma_{go}} \text{-----} (6)$$

where:

- $\Delta\rho_{og}$  is the density difference between gas and oil;
- $Z$  is the average position of the gas interface;
- $R_a$  is the average pore throat radius;
- $\sigma_{go}$  is the interfacial tension between gas and oil.

The relation is valid for three-phase coexistence for spreading oil under strong wetting conditions, but it can be applied to non-spreading of oil or other wetting conditions. For a vertical flood,  $N_B$  takes into account the balance between gravity and capillary forces and is directly proportional to the advance of the displacing phase.

Another number that can be used to describe immiscible displacements in porous media is the ratio between the two viscosities,  $M$ , as used by Lenormand et al. (1988). Horizontal displacement experiments conducted by them clearly showed that depending on the value of  $M$  and  $N_C$ , either viscous or capillary forces dominate and the displacement takes one of three basic forms:

1. Viscous fingering: the principal force is due to the viscosity of the displaced fluid; capillary effects and pressure drop in the displacing fluid are negligible.
2. Capillary fingering: at low capillary number the viscous forces are negligible in both fluids and the principal force is due to capillarity.
3. Stable displacement: the principal force is due to the viscosity of the injected fluid; capillary effects and pressure drop in the displaced fluid are negligible.

Within the three basic flow domains the patterns remained unchanged. The authors showed the validity of the three basic mechanisms by mapping values onto the plane with axes  $N_C$  and  $M$ . This mapping represents the so-called “phase diagram” for drainage. Comparison between different simulation experiments showed that changing the pore

size distribution or the size of the network leads to a translation of the boundaries, but that the general shape remains unchanged.

Miguel-Hernandez et al. (2004) developed methods of scaling dimensionless variables to simplify the analysis and thereby identify the main parameters controlling the gas-oil gravity drainage process in naturally fractured reservoirs. They developed a dimensionless group that scales time (the dimensionless time,  $t_D$ ) using a model in which gravity drainage of oil takes place through displacement by gas in the z-direction (vertical displacement) given the following conditions:

1. Constant pressure at the top and at the bottom of the matrix.
2. Flow in the vertical direction.
3. The matrix is homogeneous and isotropic.
4. There is complete phase segregation (immiscible flow).
5. The density and the viscosity are constant during displacement.
6. The potential gas gradient is approximately zero.

$$t_D = \frac{kk_{ro}^0 \Delta\rho \frac{g}{g_c}}{h\phi\mu_o (1-S_{or}-S_{wi})} t \text{-----} (7)$$

where:

- $k$  is the absolute permeability of the porous medium;
- $k_{ro}^0$  is the end-point relative oil permeability;
- $\Delta\rho$  is the density contrast between the gas and oleic phase;
- $g$  is the gravitational acceleration;
- $g_c$  is a gravitational acceleration conversion factor;
- $h$  is the height of the porous medium;
- $\phi$  is the porosity of the porous medium;
- $S_{or}$  is the residual oil saturation;
- $S_{wi}$  is the initial water saturation;
- $t$  is the injection time.

## CHAPTER 3

### EXPERIMENTAL APPARATUS AND PROCEDURE

#### 3.1 Task Formulation

To investigate the effects of wettability of the porous medium and the presence of a fracture on the GAGD performance, it was necessary to conduct several experimental runs using both water-wet and oil-wet porous media with and without a simulated vertical fracture. Within the non-fractured runs the following parameters were varied to assess their effect on the GAGD performance: (1) the mode of gas injection – secondary versus tertiary mode; (2) the method of gas displacement – constant gas pressure versus constant flow rate; and (3) the type of injection gas – N<sub>2</sub> versus CO<sub>2</sub>.

Based on the earlier work done by Sharma (2005), it was decided to keep the value of most of the parameters within the same range to be able to compare the results accordingly. Sharma conducted physical model experiments to study the effects of the gas injection mode, the gas injection method, and the gas injected on the GAGD performance, using solely water-wet porous media.

#### 3.2 Chemicals and Reagents

In the physical model experiments various chemicals and reagents of analytic grade were used. The following is a list of the chemicals used:

1. n-Decane: supplied by FischerChemicals, a division of Fischer Scientific, with a mol percentage purity of 99.9%. Molecular formula: CH<sub>3</sub>(CH<sub>2</sub>)<sub>8</sub>CH<sub>3</sub>.
2. Dimethyldichlorosilane: supplied by SUPELCO, a subsidiary of Fischer Scientific, having a purity of 99.6%. Molecular formula: (CH<sub>3</sub>)<sub>2</sub>SiCl<sub>2</sub>.
3. Methylene Chloride (dichloromethane): purchased through the University Store from different suppliers, including FischerChemicals/Fischer Scientific (HPLC grade anhydrous dichloromethane; assay: 99.9% and water: 0.004%). Molecular formula: CH<sub>2</sub>Cl<sub>2</sub>.
4. Methanol (anhydrous): purchased from Fischer Scientific. Mol percentage: >99%. Molecular formula: CH<sub>3</sub>OH.

Apart from the above listed chemicals, the author also used the following reagents:

1. Deionized water: supplied by the Water Quality Laboratory at the Louisiana State University.
2. Sudan IV red oil dye.

In the experimental setup two different kinds of porous media material were used, namely glass beads and silica sand. The glass beads (or Ballotini Solid Soda Glass Balls) were manufactured by Jencons-PLS and had the following characteristics:

- Production: Ballotini solid glass balls are produced from high quality and pure soda-lime glass. They are washed and polished without the addition of hydrofluoric acid giving them a pure shiny surface without contamination.
- Sphericity: Due to the method of manufacturing, the roundness of Ballotini cannot be guaranteed with any great accuracy. The manufacturing process and subsequent sieving of the Ballotini are both geared to the production of the most spherical Ballotini with virtual elimination of badly shaped particles.
- Diameter: In the physical model experiments ballotini with a diameter range of 0.10 to 0.20 mm were used. In the smaller diameter ranges up to 1.515 mm, approximately 80% of the material in any one grade is within the specified diameter range. Laboratory tests have shown that, for the grade used, the remaining 20% normally falls within the limits of 0.099 mm to 0.20 mm. In any consignment there may be a small percentage of irregular shaped beads which do not conform to this standard.
- Mineralogical composition:
  - SiO<sub>2</sub> 72.0%
  - Na<sub>2</sub>O 13.8%
  - CaO 9.0%
  - MgO 4.0%
  - Al<sub>2</sub>O<sub>3</sub> 1.0%
  - K<sub>2</sub>O, Fe<sub>2</sub>O<sub>3</sub> 0.2%

Silica sand was also used as material for the porous media in the physical model. The silica sand was produced by U.S. Silica Company and had the following characteristics:

- It was listed as foundry sand on the company’s website (<http://www.u-s-silica.com/PDS/Ottawa/OTTAWA%20FDY%20SANDS%202004.pdf>) and the website further states:

U. S. Silica Company supplies over 80 grades of round, angular and sub-angular sands to the foundry industry for molding and coremaking applications. Because of the high silica content and our ability to meet a wide range of sand specifications, we are helping foundry customer's produce high integrity castings, free of defects and with superior surface finishes.

- The two grades used, F-65 and F-95, had a particle size distribution as shown in Table 3.1.

**Table 3.1:** Particle Size Distribution Silica Sand (downloaded from U.S. Silica website)

	GRADE						
% RETAINED ON	F-65	F-70	F-75	F-80	F-85	F-95	F-110
30	<1						
40	3	1	<1	<1	<1	<1	
50	15	9	6	5	2	1	<1
70	29	30	24	19	12	9	4
100	31	35	38	36	38	30	18
140	18	20	25	31	38	42	44
200	3	4	6	8	9	15	25
270	<1	<1	<1	1	1	3	8
Pan						<1	<1
AFS GFN	67	70	76	80	85	95	110

- Mineralogical composition:
  - SiO<sub>2</sub>                    99.0 – 99.9%
  - Al<sub>2</sub>O<sub>3</sub>                    <0.8%
  - Fe<sub>2</sub>O<sub>3</sub>                   <0.1%
  - TiO<sub>2</sub>                     <0.1%

### 3.3 Apparatus

To study the effects of wettability and fractures on the performance of the GAGD process, a Hele-Shaw type physical model was used. The 2-D physical model consisted of two transparent plastic plates held together between two aluminum frames that were

bolted together using eighteen hex bolts. The dimensions of the plastic plates used in the model were 16" by 24" by 1". The plastic plates bounded a plastic frame containing four ports on the top, four ports on the bottom, and six ports on one side. The top and bottom ports were used as inlet and production ports, respectively, in the secondary displacement experiments. Between the plastic frame and the plastic plates, two Teflon seals were placed. The space contained within the plastic frames had a volume of 1445 cc and was used to hold the porous media during the experiments.

Besides the actual physical model the following apparatus were used:

- An electrical centrifugal pump (Brand: Lab Alliance Series 1500): the pump was used for two reasons, namely to inject water into the bottom of a pistoned transfer vessel containing n-decane in the top portion, and to inject water into the porous medium during waterflooding experiments. The pump's rate could be controlled within the range of zero to 12 cc/minute.
- A gas mass rate controller (Brand: Brooks Instruments 5850i): this device was used to control the gas injection rate during gas displacement experiments where the goal was the variation of the capillary number.
- A transfer vessel: the transfer vessel consisted of a stainless steel cylinder with a piston dividing the inner chamber in two parts. The transfer vessel was used to inject decane into the porous medium by injecting water into one chamber using the pump.

Besides the apparatus listed above, pressurized gas cylinders containing nitrogen or CO<sub>2</sub> were also used in the experiments, supplied by the Capitol Welders Supply Company, Baton Rouge, LA.

### **3.4 Experimental Procedure**

#### **3.4.1 Procedure for the Alteration of the Wettability of Glass Beads Using Dimethyldichlorosilane**

1. Measure enough glass beads for use in one test run in a large glass vessel. Prepare the glass beads for the silylation process by rinsing the glass beads with the sample solvent (methylene chloride) to remove any manufacturing residues that might interfere with the silylation process.

2. Dry the glass beads by placing them in an oven and heat them at 180°C for at least 1 hour.
3. Cool the oven to approximately 50°C and immediately place the glass beads in a 5% solution of dimethyldichlorosilane ((CH<sub>3</sub>)Cl<sub>2</sub>Si), or DMDCS, in methylene chloride (CH<sub>2</sub>Cl<sub>2</sub>). Place a piece of laboratory stretch film over the reaction vessel. Soak the glass beads in the 5% DMDCS solution for 10 minutes. Use caution when removing the glass beads from the reaction vessel because anhydrous hydrochloric acid is formed during this reaction, as demonstrated in Figure 3.1.
4. Rinse the glass beads with the same solvent used in the DMDCS solution (methylene chloride) and then soak the glass beads in methanol for 10 minutes. Once again, cover the reaction vessel with laboratory stretch film.
5. Remove the glass beads from the methanol and allow them to air dry. Once dry, the beads are thoroughly deactivated and ready for use.
6. The described procedure must be performed entirely in the fume hood using gloves, an apron, a respirator, and suitable eye protection.

#### **3.4.2 Simplified Procedure for the Wettability Alteration of Glass Beads Using Dimethyldichlorosilane**

1. Measure enough glass beads for use in one test run in a large enough glass beaker (use a glass beaker with a volume of at least 2000 cc). Prepare the glass beads for the silylation process by rinsing the glass beads with the sample solvent (methylene chloride) to remove any manufacturing residues that might interfere with the silylation process. The entire procedure must be performed in the fume hood using gloves, an apron, a respirator, and proper eye protection.
2. Place the glass beads in a 5% solution of DMDCS in methylene chloride and put a piece of laboratory stretch film over the reaction vessel. Soak the glass beads in the 5% DMDCS solution for 10 minutes. Use caution when removing the glass beads from the reaction vessel because anhydrous hydrochloric acid is formed during this reaction (see Figure 3.1).
3. Rinse the glass beads with the same solvent used in the DMDCS solution (methylene chloride) and then soak the glass beads in methanol for 10 minutes. Once again cover the reaction vessel with laboratory stretch film.

- Remove the glass beads from the methanol. Allow the treated beads to air dry for thirty minutes. Afterwards, dry the glass beads thoroughly in an oven at 150 °C for at least four hours.

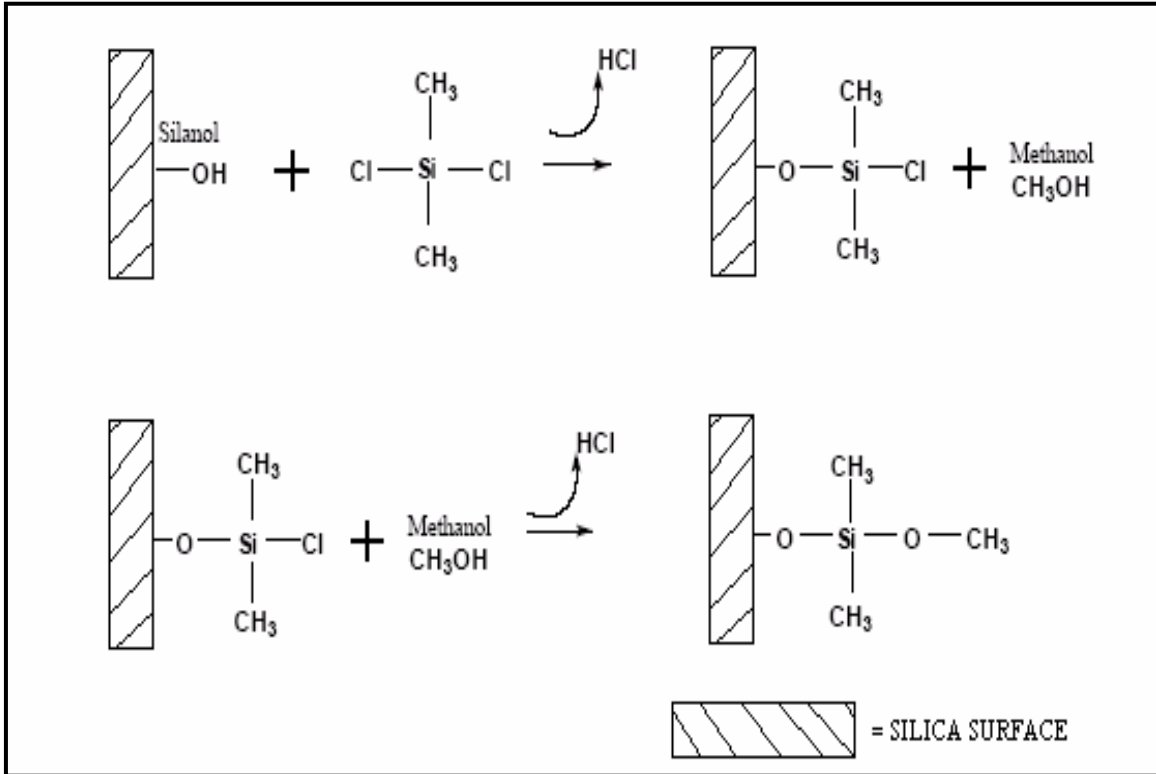


**Figure 3.1:** Reaction Mechanism of the Wettability Alteration Procedure

### 3.4.3 Modified Procedure for the Amott Test

A modified Amott test was performed on treated glass beads and silica sand according to the following procedure:

- Imbibe water into the prepared physical model using a burette and demineralized water. Once the model is completely saturated with water, record the volume of water imbibed to calculate the bulk pore volume.
- Displace the water with n-decane using the transfer vessel and the centrifugal pump at a constant rate of 3 cc/min. Use a graduated glass cylinder to collect any effluent liquid during the water displacement. The end of the oil flood is reached when no more water is produced and collected in the graduated cylinder. Stop the pump.

3. Calculate the connate water saturation and the initial oil saturation using material balance equations.
4. Perform a waterflood by first placing the physical model horizontal (non gravity-stable waterflood) and then injecting water into it with the centrifugal pump at a rate of 3 cc/min. Collect all produced liquids in a graduated cylinder and when no more oil is produced, the waterflood is ended by stopping the pump.
5. Calculate the residual oil saturation after the waterflood using mass balance equations.
6. Connect all of the ports to burettes filled with n-decane and let stand for 20 hours. Measure the volume of water displaced through spontaneous water imbibition.
7. Conduct a second oil flood using the transfer vessel and the centrifugal pump at a constant rate of 3 cc/min. Use a graduated glass cylinder to collect any effluent liquid during the water displacement. The end of the oil flood is reached when no more water is produced and collected in the graduated cylinder. Stop the pump.
8. Calculate the connate water saturation and the initial oil saturation using material balance equations.
9. Connect all of the ports to burettes filled with demineralized water and let stand for 20 hours. Measure the volume of oil displaced through spontaneous oil imbibition.
10. Perform a second waterflood by placing the physical model horizontal (non gravity-stable waterflood) and injecting water into it with the centrifugal pump at a rate of 3 cc/min. Collect all produced liquids in a graduated cylinder. When no more oil is produced, end the waterflood by stopping the pump.
11. Calculate the residual oil saturation after the waterflood using mass balance equations.
12. Calculate  $\delta_o$  and  $\delta_w$  using equations 3a and 3b (see § 2.4.2).

#### **3.4.4 Preparation of the Pistoned Transfer Vessel**

At the start of every experimental run, the transfer vessel was filled with n-decane. The chamber containing the water was first evacuated by connecting the decane side to a high-pressure nitrogen cylinder and using the pressurized gas to push down the piston and drive out the water. The decane side was then opened up, cleaned thoroughly using

acetone, and filled with n-decane dyed red with the oil dye. After closing the transfer vessel securely, it was ready to be used in the experiments.

### 3.4.5 Preparing the Porous Medium

Each experimental run was conducted using a newly prepared porous medium (bead or sand pack). First, the physical model was assembled taking care to tighten the bolts using a torque wrench in numerical order (1 to 18). A torque of 60 lbs-in, at maximum, was put on the bolts to assure that a proper sealing of the model was achieved. The model was then filled with the appropriate porous medium (glass beads or silica sand) using the top ports and the help of a glass funnel. The filling method can be characterized as a pour-and-tap filling, meaning that the beads or sand grains were poured into the model under contiguous tapping to ensure a homogeneous and close packing of the glass beads or silica sand. To further ensure that the model had a vacuum-tight seal, vacuum was applied to it using a vacuum pump after filling and tested for an hour to check for leaks.

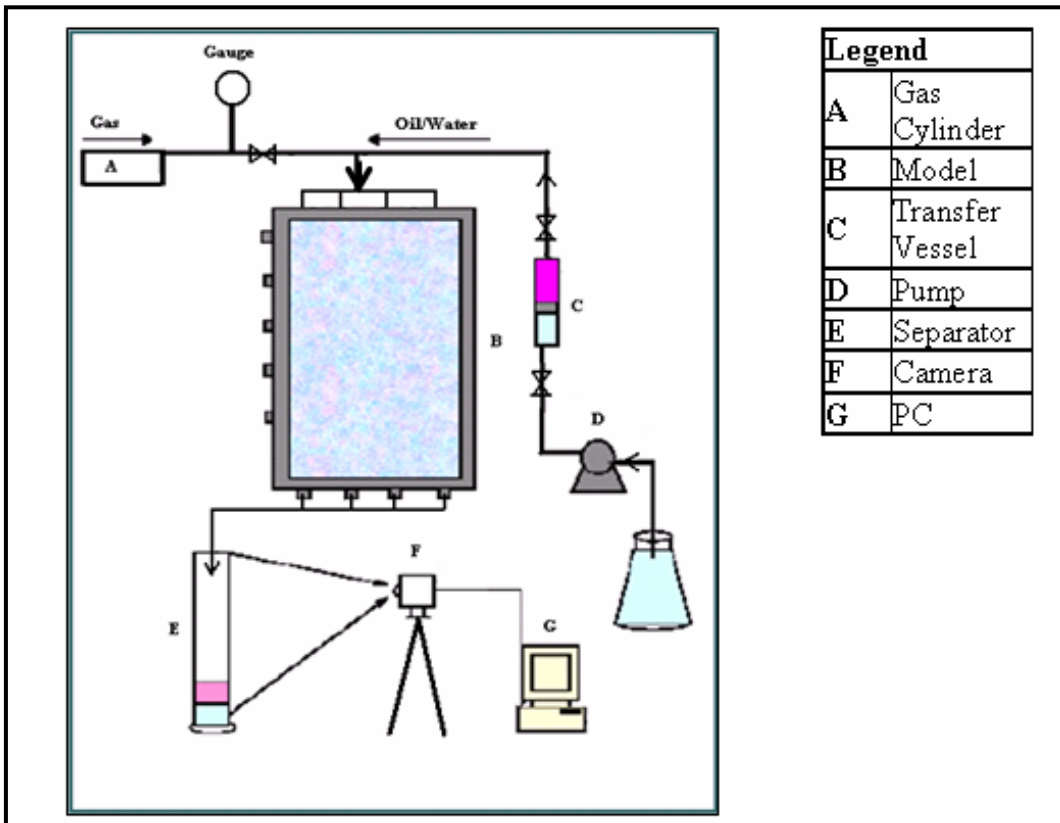


**Figure 3.2:** Schematic Diagram of Experimental Setup

### **3.4.6 Initiating the Gas Displacement Experiments**

During the gas displacement experiments the produced liquids were carefully monitored and recorded using a LabView data acquisition system (see Figure 3.2). This was done through the use of a camera that recorded the fluid levels in the glass separator in which the produced liquids were collected. The steps to initiate the LabView data acquisition system were as follows:

1. Start the Data Acquisition software.
2. Choose to acquire a new image and adjust the image settings until the picture is satisfactory. Return and save the acquired image.
3. Choose the “Simple Calibration” from the “Image” options menu. Set the calibration coordinates and the correct pixel settings.
4. Use the “Edge Detector” option from the “Calibrate” menu to find the fluid levels in the separator. The “Caliper” option is then used to select the measurement of the appropriate fluid levels.
5. Use the “Create LabView Script” under the “Script” options to create a new script to be used in the LabView program. Choose the “Image Board” option when creating the script file.
6. When the Image Board opens, use the “Connector Tool” to connect the read-out grid to the script icon. Save under an appropriate filename.
7. Open the correct vision system script in the LabView program and replace the “Image Board” script with the one just created using the “Diagram” view.
8. Type in the name of the output file that will be created during the displacement experiments to record the fluid levels throughout the experiment.
9. Hit the “Run” button.

### **3.4.7 Procedure for Conducting the Secondary Displacement Experiments**

The secondary mode displacement experiments were consistently conducted with the following steps as a guideline:

1. Prepare the transfer vessel.
2. Assemble the physical model and pack the porous medium.

3. Imbibe water into the bead or sand pack using a burette and demineralized water. Once the model is completely saturated with water, record the volume of water imbibed to calculate the bulk pore volume.
4. Displace the water with n-decane using the transfer vessel and the centrifugal pump at a constant rate of 3 cc/min. Use a graduated glass cylinder to collect any effluent liquid during the water displacement. The end of the oil flood is reached when no more water is produced and collected in the graduated cylinder. Stop the pump.
5. Calculate the connate water saturation and the initial oil saturation using material balance equations.
6. Initiate the gas injection and leave the experiment running for a period of at least 24 hours to ensure thorough displacement and drainage of the fluids. Collect any produced fluids in the glass separator and record the fluid levels using the LabView data acquisition system.
7. Constant pressure experiments: Perform the gas injection by using a pressurized gas cylinder and a gas pressure regulator with a pressure gauge in the injection line to ensure that the proper value of the gas pressure is used.
8. Constant rate experiments: Conduct the gas displacement by using the gas mass rate controller along with a pressurized gas cylinder.
9. Calculate the oil recovery using mass balance equations.

When conducting the fracture simulation experiments, all of the steps above apply, except that the fracture simulation needs to be placed in the plastic frame prior to the assembly and filling of the physical model.

#### **3.4.8 Procedure for Conducting the Tertiary Displacement Experiments**

The tertiary mode displacement experiments are very similar to the secondary mode experiments except that a waterflood precedes the gas injection. The tertiary mode experiments were run according to the following steps:

1. Prepare the transfer vessel.
2. Assemble the physical model and pack the porous medium.
3. Imbibe water into the bead or sand pack using a burette and demineralized water.
4. Displace the water with n-decane using the transfer vessel and the centrifugal pump at a constant rate of 3 cc/min. Use a graduated glass cylinder to collect any effluent

liquid during the water displacement. The end of the oil flood is reached when no more water is produced and collected in the graduated cylinder. Stop the pump.

5. Calculate the connate water saturation and the initial oil saturation using material balance equations.
6. Perform a waterflood by first placing the physical model horizontal (non gravity-stable waterflood) and inject water into it with the centrifugal pump at a rate of 3 cc/min. Collect all produced liquids in a graduated cylinder and when no more oil is produced, end the waterflood by stopping the pump.
7. Calculate the residual oil saturation after the waterflood using mass balance equations.
8. Return the physical model to a vertical position making sure that the oil bank is on top.
9. Initiate the gas injection and leave the experiment running for at least 24 hours to ensure thorough displacement and drainage of the fluids. Collect any produced fluids in the glass separator and monitor the fluid levels using the LabView data acquisition system.
10. Constant pressure experiments: Conduct the gas injection by using a pressurized gas cylinder and a gas pressure regulator with a pressure gauge in the injection line to assure that the proper value of the gas pressure is used.
11. Constant rate experiments: Perform the gas displacement by using the gas mass rate controller along with a pressurized gas cylinder.
12. Calculate the oil recovery using mass balance equations.

### **3.5 Overview of the Conducted Experiments**

In the first series of experiments the effect of the wettability on the GAGD performance was the focus. A total of six 2-D water-wet GAGD experiments were conducted during this study:

1. CP-S-WW-13-1: Constant pressure (4 psig), secondary mode, water-wet silica sand with an average diameter of 0.13 mm. Gas: N<sub>2</sub>.
2. CF-S-WW-13-1: Constant mass flow rate (300 cc/min), secondary mode, water-wet silica sand with an average diameter of 0.13 mm. Gas: N<sub>2</sub>.

3. CP-S-WW-15-1: Constant pressure (4 psig), secondary mode, water-wet glass beads with an average diameter of 0.15 mm. Gas: N<sub>2</sub>.
4. CP-T-WW-13-3: Constant pressure (4 psig), tertiary mode, water-wet silica sand with an average diameter of 0.13 mm. Gas: N<sub>2</sub>.
5. CP-T-WW-13-4: Constant pressure (4 psig), tertiary mode, water-wet silica sand with an average diameter of 0.13 mm. Gas: N<sub>2</sub>.
6. CP-T-WW-15-1: Constant pressure (4 psig), tertiary mode, water-wet glass beads with an average diameter of 0.15 mm. Gas: N<sub>2</sub>.

Thirteen 2-D oil-wet GAGD experiments were also conducted during this study. Eight were run in the secondary mode and five were conducted in the tertiary recovery mode:

1. CP-S-OW-13-1: Constant pressure (4 psig), secondary mode, oil-wet silica sand with an average diameter of 0.13 mm. Gas: N<sub>2</sub>.
2. CP-S-OW-13-2: Constant pressure (4 psig), secondary mode, oil-wet silica sand with an average diameter of 0.13 mm. Gas: CO<sub>2</sub>.
3. CP-S-OW-13-3: Constant pressure (4 psig), secondary mode, oil-wet silica sand with an average diameter of 0.13 mm. Gas: N<sub>2</sub>.
4. CP-S-OW-15-1: Constant pressure (4 psig), secondary mode, oil-wet glass beads with an average diameter of 0.15 mm. Gas: N<sub>2</sub>.
5. CP-S-OW-15-2: Constant pressure (4 psig), secondary mode, oil-wet glass beads with an average diameter of 0.15 mm. Gas: N<sub>2</sub>.
6. CP-S-OW-60-1: Constant pressure (4 psig), secondary mode, oil-wet silica sand with an average diameter of 0.60 mm. Gas: N<sub>2</sub>.
7. CF-S-OW-13-1: Constant mass flow rate (75 cc/min), secondary mode, oil-wet silica sand with an average diameter of 0.13 mm. Gas: N<sub>2</sub>.
8. CF-S-OW-13-2: Constant mass flow rate (75 cc/min), secondary mode, oil-wet silica sand with an average diameter of 0.13 mm. Gas: CO<sub>2</sub>.
9. CP-T-OW-13-1: Constant pressure (4 psig), tertiary mode, oil-wet silica sand with an average diameter of 0.13 mm. Gas: N<sub>2</sub>.
10. CP-T-OW-13-2: Constant pressure (4 psig), tertiary mode, oil-wet silica sand with an average diameter of 0.13 mm. Gas: N<sub>2</sub>.

11. CP-T-OW-15-1: Constant pressure (4 psig), tertiary mode, oil-wet glass beads with an average diameter of 0.15 mm. Gas: N<sub>2</sub>.
12. CP-T-OW-15-2: Constant pressure (4 psig), tertiary mode, oil-wet glass beads with an average diameter of 0.15 mm. Gas: N<sub>2</sub>.
13. CF-T-OW-13-2: Constant mass flow rate (300 cc/min), tertiary mode, oil-wet silica sand with an average diameter of 0.13 mm. Gas: N<sub>2</sub>.

In the subsequent series of experiments, the simulation of a fracture and its effect on the oil recovery was of importance:

1. CP-S-WW-13-1-F: Constant pressure (4 psig), secondary mode, water-wet silica sand with an average diameter of 0.13 mm. Gas: N<sub>2</sub>. Fracture simulation.
2. CP-S-WW-13-2-F: Constant pressure (4 psig), secondary mode, water-wet silica sand with an average diameter of 0.13 mm. Gas: N<sub>2</sub>. Fracture simulation.

The last series of experiments were an attempt to simulate the presence of a vertical fracture in the porous medium and to study its effect on the GAGD oil recovery. A total of seven experiments were conducted using two different grain sizes in two different wettability states:

1. CP-S-WW-13-1-F: Constant pressure (4 psig), secondary mode, water-wet silica sand with an average diameter of 0.13 mm. Gas: N<sub>2</sub>. Fracture simulation.
2. CP-S-WW-13-2-F: Constant pressure (4 psig), secondary mode, water-wet silica sand with an average diameter of 0.13 mm. Gas: N<sub>2</sub>. Fracture simulation.
3. CP-S-OW-13-1-F: Constant pressure (4 psig), secondary mode, oil-wet silica sand with an average diameter of 0.13 mm. Gas: N<sub>2</sub>. Fracture simulation.
4. CP-S-OW-13-2-F: Constant pressure (4 psig), secondary mode, oil-wet silica sand with an average diameter of 0.13 mm. Gas: N<sub>2</sub>. Fracture simulation.
5. CP-S-WW-15-1-F: Constant pressure (4 psig), secondary mode, water-wet glass beads with an average diameter of 0.15 mm. Gas: N<sub>2</sub>. Fracture simulation.
6. CP-S-WW-15-2-F: Constant pressure (4 psig), secondary mode, water-wet glass beads with an average diameter of 0.15 mm. Gas: N<sub>2</sub>. Fracture simulation.
7. CP-S-OW-15-1-F: Constant pressure (4 psig), secondary mode, oil-wet glass beads with an average diameter of 0.15 mm. Gas: N<sub>2</sub>. Fracture simulation.

The general key to the nomenclature used to identify the experiments is:

### **AB-C-DE-nn-m-X**

with:

1. AB: Denotes the method of gas displacement – CP = constant pressure; CF = constant flow rate.
2. C: Denotes the strategy used for the gas injection – S = secondary mode gas injection; T = tertiary mode gas injection.
3. nn: These two digits refer to the average grain size diameter of the porous medium used – 13 = 0.13 mm, 15 = 0.15 mm, 60 = 0.60 mm.
4. m: The single digit refers to the run number.
5. X: Refers to any special features of the experimental run – F = fracture simulation.

## CHAPTER 4

### RESULTS AND DISCUSSION

To confirm the wettability alteration by the treatment with DMDCS, a modified Amott test was performed on treated glass beads and silica sand. The results of the Amott test will be presented in the first section.

In this study the effect of the wettability of the porous medium and the presence of a fracture on the performance of the GAGD process was investigated. To that extent, various gas displacement runs were conducted using both water-wet and oil-wet porous media while varying such parameters as strategy of gas injection, method of gas displacement, the type of gas injected, and the simulation of a vertical fracture in the physical model. The results of this study are summarized in the following sections, and the dimensionless numbers, characteristic of the experiments, will be examined in the last part of this chapter.

#### 4.1 The Confirmation of the Wettability Alteration

During the experiments the first means of confirmation of the wettability were visual ones. The wettability state of the porous media used was visually confirmed during the oil flooding part of the experimental procedure. The water-wet porous media always displayed a “mottled” appearance (i.e., the oil did not displace the water uniformly resulting in a swept red area speckled with unswept whiter portions). The oil-wet porous media, however, consistently showed a characteristic homogeneously red area indicating that the water was uniformly displaced by the injected n-decane (see Figure 4.1).

To quantitatively confirm the wettability state of the porous media used, a modified Amott test was conducted on the treated porous media material. The results of the modified Amott test can be summarized as follows:

##### 1. Oil-wet 0.13 mm silica sand:

Pore volume = 456 cc

Oil in cell = 368.7 cc

$V_{wsp} = 5$  cc

$V_{wt} = 255$  cc

Oil in cell after waterflood = 110.5 cc

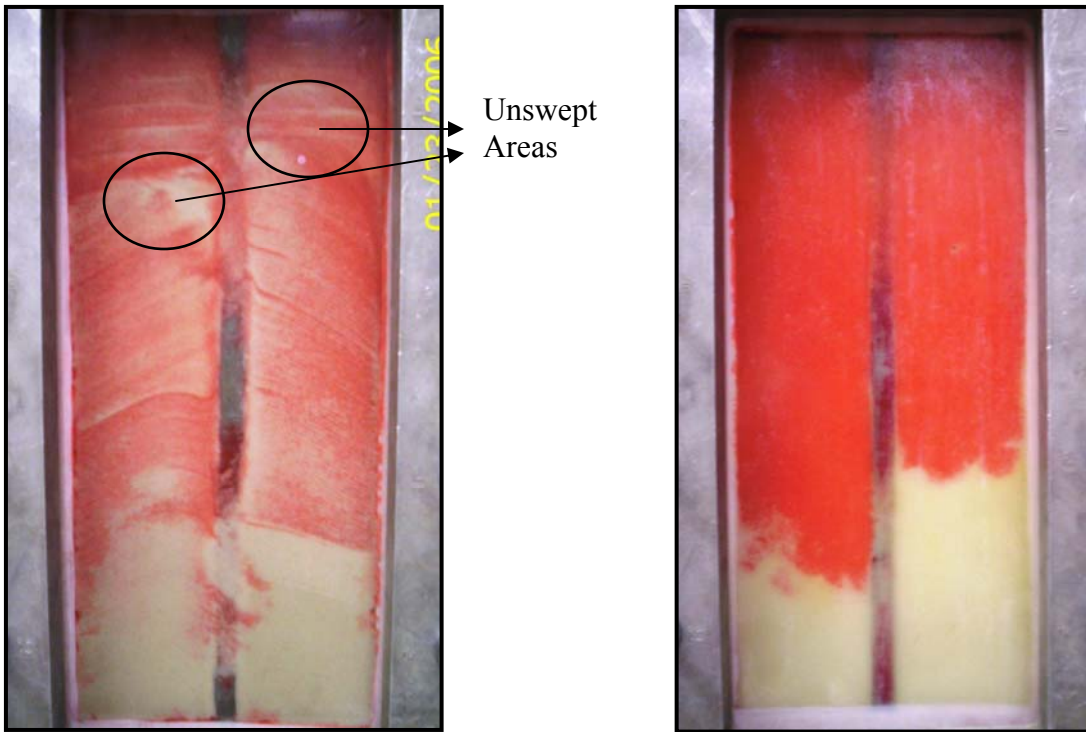


**Figure 4.1:** Visual Comparison of Water-Wet Porous Medium (Left) with Oil-Wet Porous Medium (Right) During Oil Flooding

Oil in cell after oil flood = 365.5 cc

$V_{osp} = 7.3$  cc

$V_{ot} = 224.9$  cc

$\delta_o = V_{wsp}/V_{wt} = 5/255 = 0.0196$

$\delta_w = V_{osp}/V_{ot} = 7.3/224.9 = 0.0325$

**2. Oil-wet 0.15 mm glass beads:**

Pore volume = 504 cc

Oil in cell = 461.7 cc

$V_{wsp} = 4.4$  cc

$V_{wt} = 225$  cc

Oil in cell after waterflood = 293.9 cc

Oil in cell after oil flood = 518.9 cc

$V_{osp} = 1.0$  cc

$V_{ot} = 248.6$  cc

$\delta_o = V_{wsp}/V_{wt} = 4.4/225 = 0.0196$

$$\delta_w = V_{osp}/V_{ot} = 1.0/248.6 = 0.0040$$

According to the criteria of the Amott test, an oil wet porous medium has a positive displacement-by-oil ratio,  $\delta_o$ , and zero displacement-by-water ratio,  $\delta_w$ . Because of the high porosity (36-39 %) and permeability (2,000-5,000 mD) of the sand and bead packs used in these tests, the Amott tests were inconclusive due to the negligible capillary forces needed for imbibition.

The confirmation of the wettability state of the porous media used was finally provided by the fractional flow curves (see Figures 4.2 and 4.3). They exhibit the characteristic shift to the left of the fractional flow curve of the oil-wet silica sand or glass beads compared to the water-wet fractional flow curve. The fractional flow curves were calculated according to the method as outlined by Johnson et al. (1957).

## **4.2 The Effect of Wettability on GAGD Performance**

The first series of experiments focused on the effect of the wettability on the GAGD performance, and, as such, it was deemed important to vary the following parameters during the gas displacement experiments:

1. The strategy of gas injection – secondary mode or tertiary mode.
2. The method of gas displacement – constant pressure gas displacement or constant mass rate gas displacement.
3. The type of gas injected –  $N_2$  or  $CO_2$ .

The second series of experiments was geared towards investigating the effect of a fracture in the porous medium on the oil recovery and will be discussed in section 4.3.

### **4.2.1 The Secondary Mode Gas Displacement Experiments**

#### **4.2.1.1 Discussion of the Results**

The objective of the first series of 2-D physical model experiments was to study the effect of the wettability of the porous medium on the GAGD performance. The results for the secondary mode experiments within that first series are summarized in Tables 4.1-3. The parameters that were varied in the secondary mode experiments were: the wettability state of the porous media, the average grain size of the porous media, the method of gas displacement, and the type of gas injected.

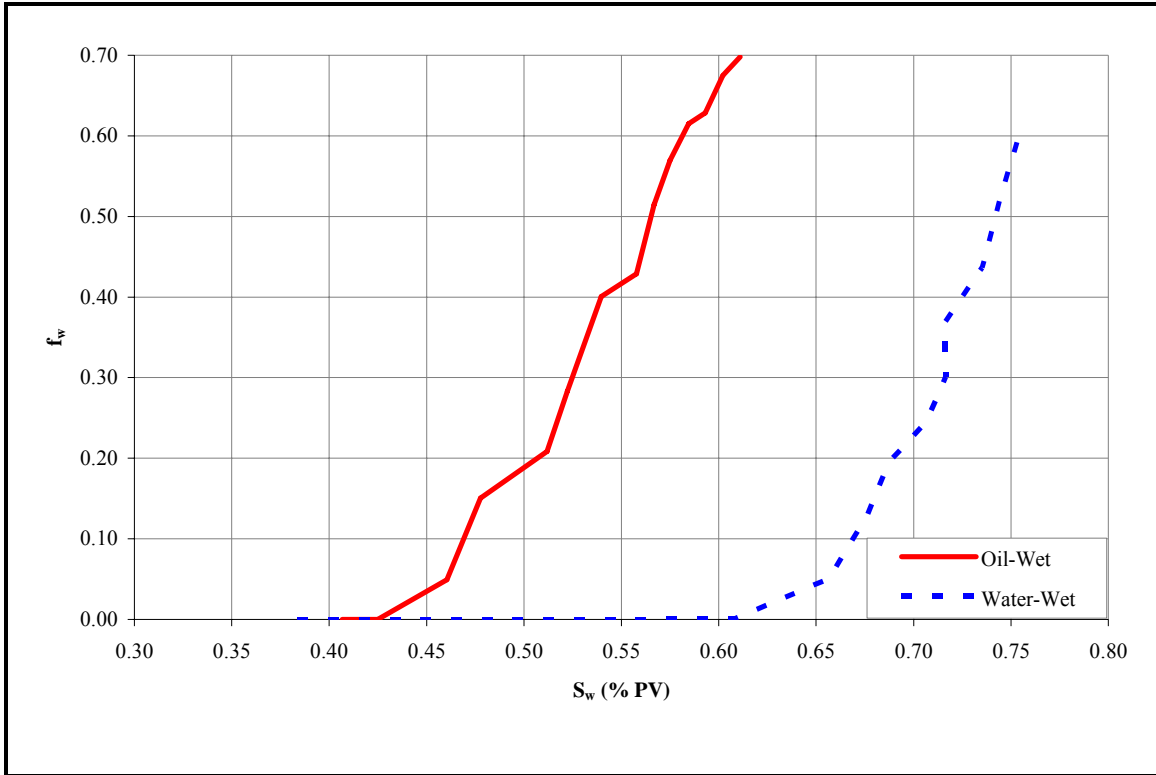


**Figure 4.2:** Fractional Flow Curves for the 0.13 mm Silica Sand

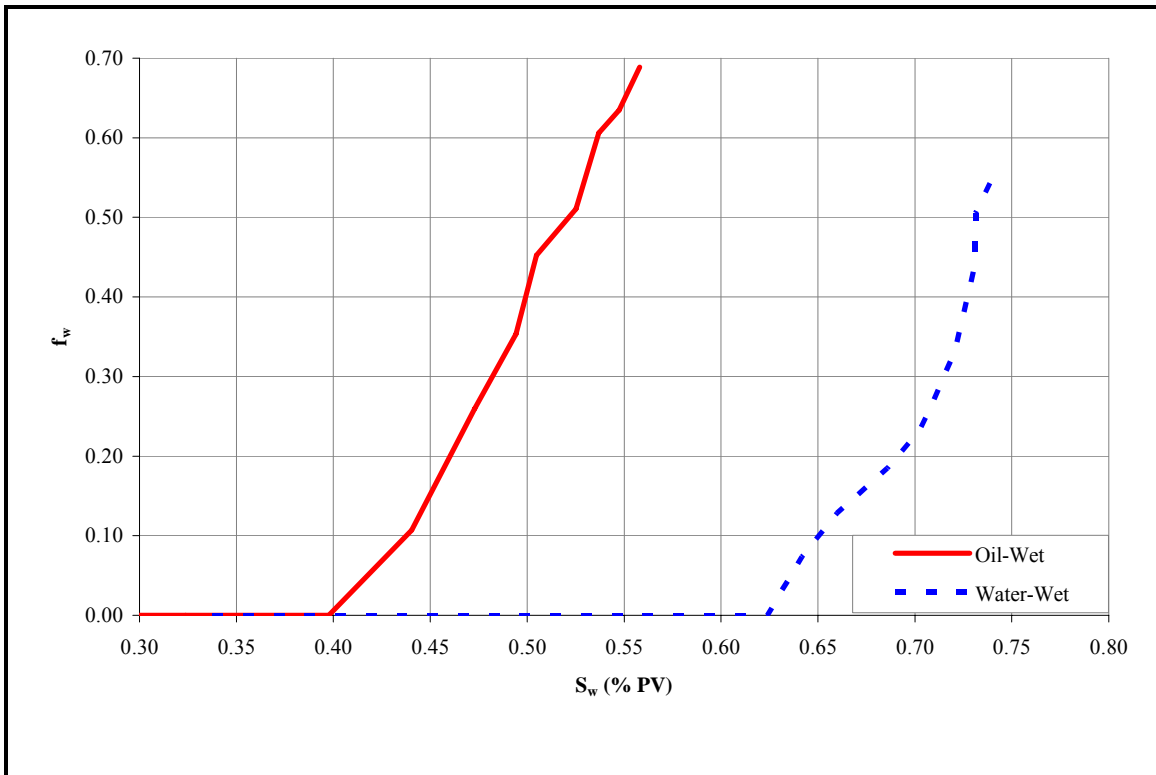


**Figure 4.3:** Fractional Flow Curves for the 0.15 mm Glass Beads

**The type of gas injected:**

From the results (Figure 4.4), it appears that the type of injection gas does affect the oil recovery of the secondary mode experiment. Whenever CO<sub>2</sub> was used as the displacement gas the oil recoveries were found to be higher than when N<sub>2</sub> was used. An increase in oil recovery of 10.9 % of the original oil in place (OOIP) is achieved in the CO<sub>2</sub> experiments. This difference can probably be attributed to the effect of CO<sub>2</sub> on oil: the high solubility of CO<sub>2</sub> in oil causes the oil to swell thereby increasing its saturation and relative permeability, which results in significantly enhancing the oil recovery by improving the oil “flowability” (Darvish et al., not dated).

**The method of gas displacement:**

According to Muskat (1981):

The gas injection serves mainly to maintain the reservoir pressure, prolong the flowing life, and to provide high flow capacities. It is only to the extent that that these conditions facilitate operations under which gravity drainage can be effective that pressure maintenance indirectly also represents an important contributing factor to high recovery by gravity drainage. (p. 494)

This only confirms what is evident when we compare the results from the constant pressure runs with those from the constant rate runs: the constant pressure runs using nitrogen as the injected gas show an increase of up to 3 %OOIP in the oil recovery (see Figure 4.5).

**The average grain size of the porous medium:**

Permeability and variations in permeability (heterogeneity) are considered to be of vital importance to the success of many hydrocarbon recovery processes (Panda & Lake, 1994). The Carmen-Kozeny equation provides a quantitative connection between textural properties, such as grain size, sorting and packing, and single phase permeability. For the special case of an assembly of single-size spheres of diameter, the Carmen-Kozeny equation for the absolute permeability (k) of a porous medium becomes:

$$k = \frac{D_p^2 \phi^3}{72\tau(1-\phi)^2} \text{-----} (8)$$

**Table 4.1:** Model Parameters for the Water-Wet Runs in Secondary Mode

Model Parameters	CP-S-WW-13-1	CF-S-WW-13-1	CP-S-WW-15-1
Gas	N <sub>2</sub>	N <sub>2</sub>	N <sub>2</sub>
P (psig)	4	N/A	4
Rate (cc/min)	N/A	300	N/A
D <sub>g</sub> (mm)	0.13	0.13	0.15
<b>INITIAL CONDITIONS</b>			
Pore Volume (cc)	524	528	558
Oil Flood Water (cc)	362.8	362.8	372.8
OOIP (cc)	362.8	362.8	372.8
Porosity $\phi$ (%)	36.5	36.5	38.6
S <sub>wc</sub> (%)	30.8	31.3	33.2
S <sub>oi</sub> (%)	69.2	68.7	66.8
<b>GAS INJECTION</b>			
k (Darcy)	4.7	4.9	8.1
Recovery (% OOIP)	66.7	60.1	72.7

**Table 4.2:** Model Parameters for the Oil-Wet Runs in Secondary Mode – Constant Pressure Runs

Model Parameters	CP-S-OW-13-1	CP-S-OW-13-2	CP-S-OW-13-3	CP-S-OW-15-1	CP-S-OW-15-2	CP-S-OW-60-1
Gas	N <sub>2</sub>	CO <sub>2</sub>	N <sub>2</sub>	N <sub>2</sub>	N <sub>2</sub>	N <sub>2</sub>
P (psig)	4	4	4	4	4	4
Rate (cc/min)	N/A	N/A	N/A	N/A	N/A	N/A
D <sub>g</sub> (mm)	0.13	0.13	0.13	0.15	0.15	0.60
<b>INITIAL CONDITIONS</b>						
Pore Volume (cc)	528	531	571.5	476	504.0	516.0
Oil Flood Water (cc)	357.8	450.5	475.5	347.7	455.5	433.7
OOIP (cc)	357.8	450.5	475.5	347.7	455.5	433.7
Porosity $\phi$ (%)	36.5	36.7	39.6	32.9	34.9	35.7
S <sub>wc</sub> (%)	32.2	15.2	16.8	27.0	9.6	15.9
S <sub>oi</sub> (%)	67.8	84.8	83.2	73.0	90.4	84.1
<b>GAS INJECTION</b>						
k (Darcy)	4.9	5.2	7.3	4.2	5.3	0.8
N <sub>B</sub>	6.6E-06	7.4E-06	9.1E-06	6.3E-06	7.5E-06	6.0E-06
N <sub>C</sub>	3.1E-07	3.2E-07	5.3E-06	3.0E-07	5.7E-07	6.3E-07
N <sub>G</sub>	20.9	23.4	17.0	21.3	15.8	9.6
Recovery (% OOIP)	77.7	86.7	74.0	78.6	83.6	81.6

**Table 4.3:** Model Parameters for the Oil-Wet Runs in Secondary Mode – Constant Flow Rate Runs

Model Parameters	CF-S-OW-13-1	CF-S-OW-13-2
Gas	N <sub>2</sub>	CO <sub>2</sub>
P (psig)	N/A	N/A
Rate (cc/min)	75	75
D <sub>g</sub> (mm)	0.13	0.13
<b>INITIAL CONDITIONS</b>		
Pore Volume (cc)	576	535
Oil Flood Water (cc)	475.5	415.5
OOIP (cc)	475.5	415.5
Porosity $\phi$ (%)	39.9	37.0
S <sub>wc</sub> (%)	17.4	22.3
S <sub>oi</sub> (%)	82.6	77.7
<b>GAS INJECTION</b>		
k (Darcy)	7.3	5.2
N <sub>B</sub>	9.5E-06	7.2E-06
N <sub>C</sub>	4.7E-06	4.7E-06
N <sub>G</sub>	2.0	1.5
Recovery (% OOIP)	74.7	92.8

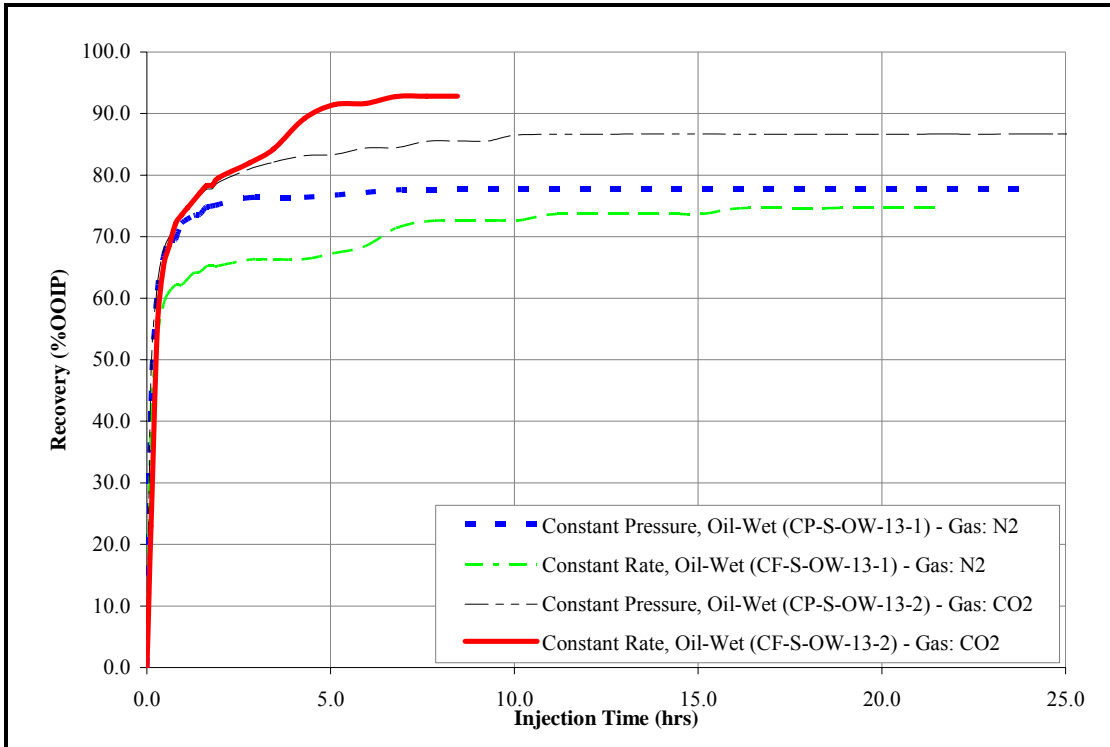


**Figure 4.4:** Effect of the Injected Gas on the Oil Recovery – Secondary Mode Runs

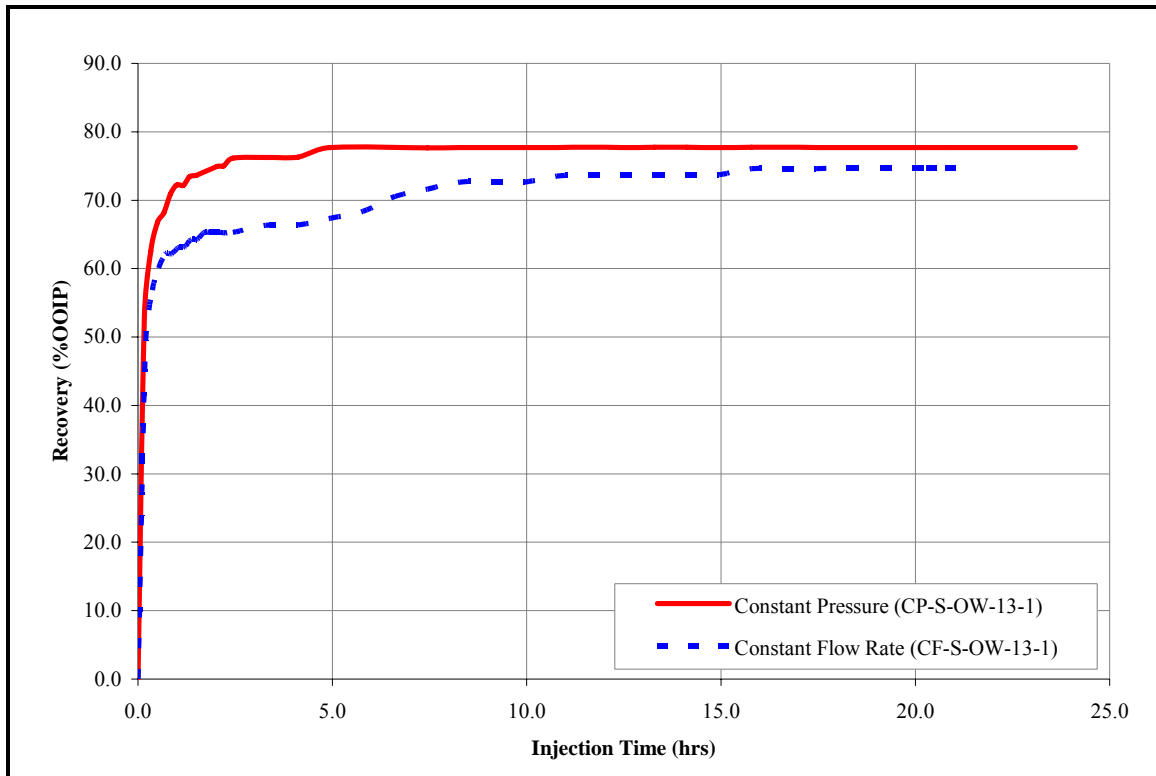


**Figure 4.5:** Effect of the Gas Injection Method on the Oil Recovery – Secondary Mode Runs, Oil-Wet Case, 0.13 mm Sand Pack

with:  $D_p$  = the grain size diameter;  $\phi$  = the porosity of the porous medium; and  $\tau$  = the tortuosity of the flow path through the porous medium.

This equation implies that an increase of the average grain diameter of the porous medium will lead to an increase in the permeability and, therefore, a potential increase in the effectiveness of the GAGD process. The experiments show that an increase in the grain size diameter does indeed result in an increase in the oil recovery (see Figure 4.6).

**The wettability of the porous medium:**

As mentioned in the literature review, gravity drainage promises to be a very effective enhanced oil recovery method in oil-wet reservoirs because the oil phase is always present as a continuous film on the pore walls, thus resulting in potentially very low residual oil saturations.

This also comes through in the experimental results: the change in wettability from water-wet to oil-wet appears to significantly improve the oil recovery, as can be seen

from Figures 4.7 – 4.9. The incremental production over the corresponding water-wet cases can be summarized as follows:

- Constant pressure secondary runs, 0.13 mm: +9.2 %OOIP.
- Constant pressure secondary runs, 0.15 mm: +8.4 %OOIP.
- Constant rate secondary runs, 0.13 mm: +14.6 %OOIP.

See Table 4.6 for a complete summary of the incremental effect on the oil recovery.

## **4.2.2 The Tertiary Mode Gas Displacement Experiments**

### **4.2.2.1 The Experimental Results**

The results of the 2-D GAGD experiments in tertiary mode are shown in Tables 4.4 and 4.5.

### **4.2.2.2 Discussion of the Results**

The most important difference between secondary and tertiary gas displacement processes is the presence of mobile water, which can lead to increased water shielding and water handling problems in commercial gas injection projects (Sharma, 2005).

As with the secondary mode gas displacement experiments, certain variables were varied during the tertiary runs to ascertain their effect on the GAGD performance, namely: the wettability of the porous medium, the average grain size of the particles in the porous medium, and the method of gas displacement.

In the experiments the waterflood was conducted using demineralized water at a displacement rate of 3 cc/min.

#### **The method of gas displacement:**

The results from the tertiary mode experiments wherein the method of gas displacement was varied were similar to those conducted without a waterflood with regards to the higher oil recovery gained in the constant pressure runs as opposed to the constant rate runs (see Figure 4.10). On average, the oil recovery increased by 6.8 % of the residual oil in place (ROIP) or 5.6 % of the original oil in place (OOIP).

#### **The average grain size:**

Even though an increase in the oil recovery in the tertiary mode experiments using larger glass beads was expected, the results show that the contrary happened, as shown in Table 4.5.

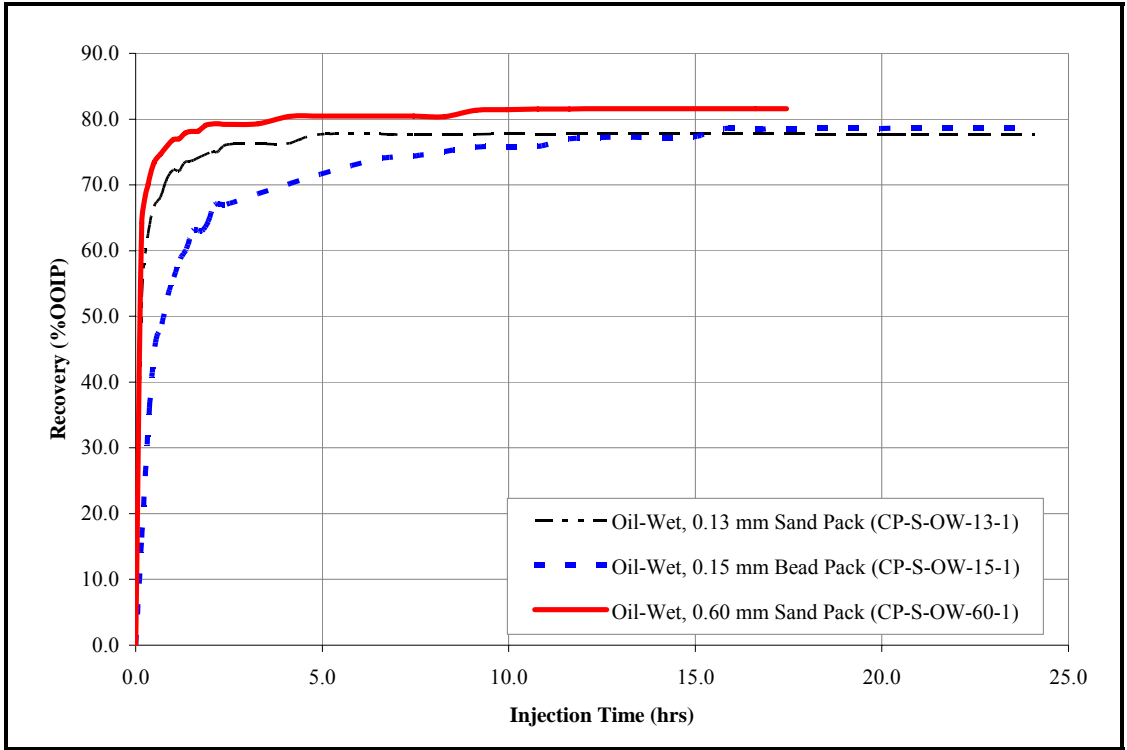


**Figure 4.6:** Effect of Average Grain Size on the Oil Recovery – Secondary Mode Runs

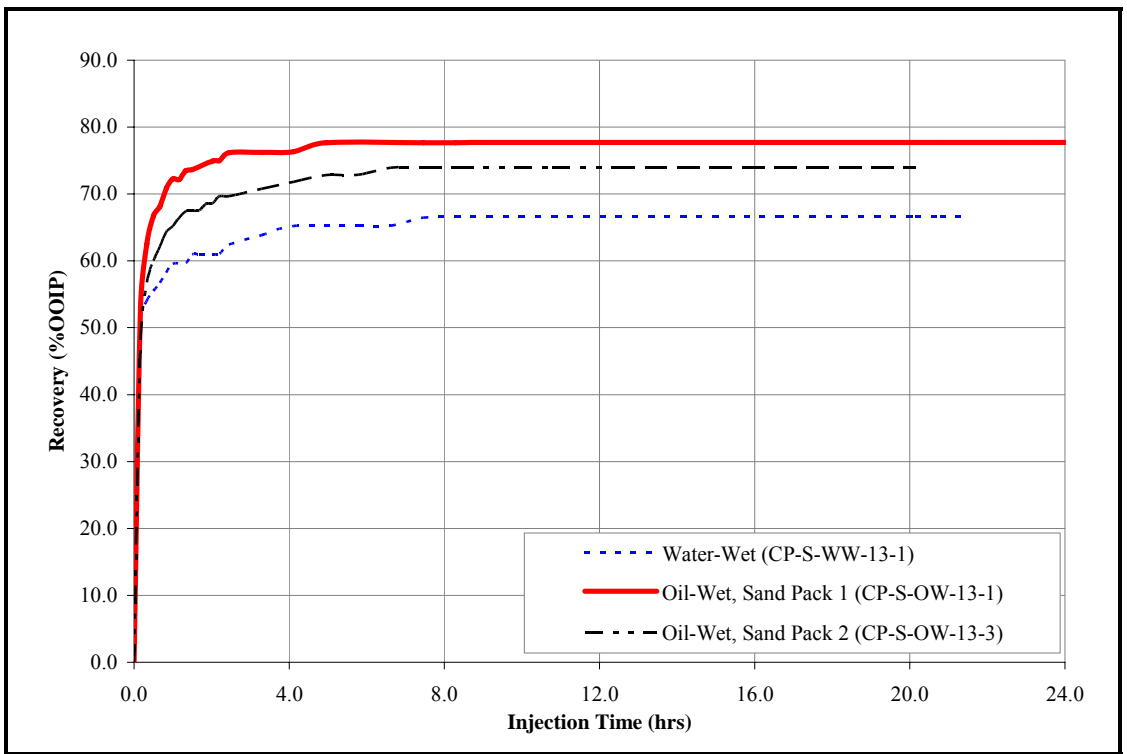


**Figure 4.7:** Effect of the Wettability on the Oil Recovery – Secondary Mode, Constant Pressure, 0.13 mm Sand Pack

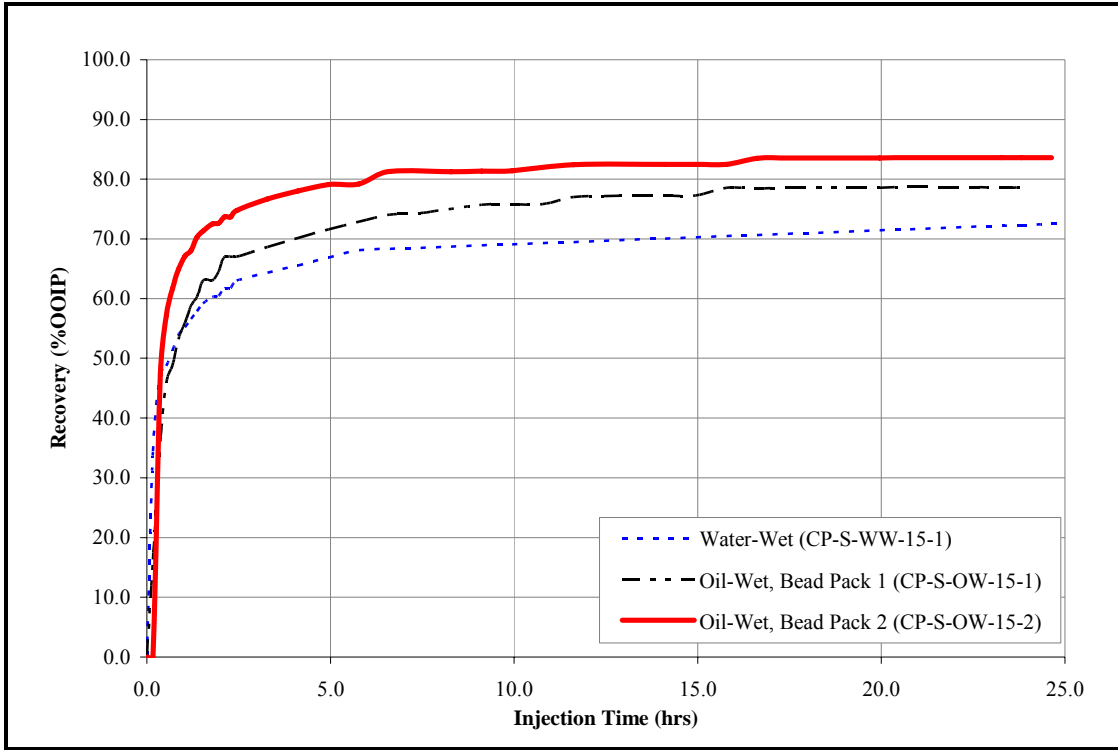


**Figure 4.8:** Effect of the Wettability on the Oil Recovery – Secondary Mode, Constant Pressure, 0.15 mm Glass Bead Pack

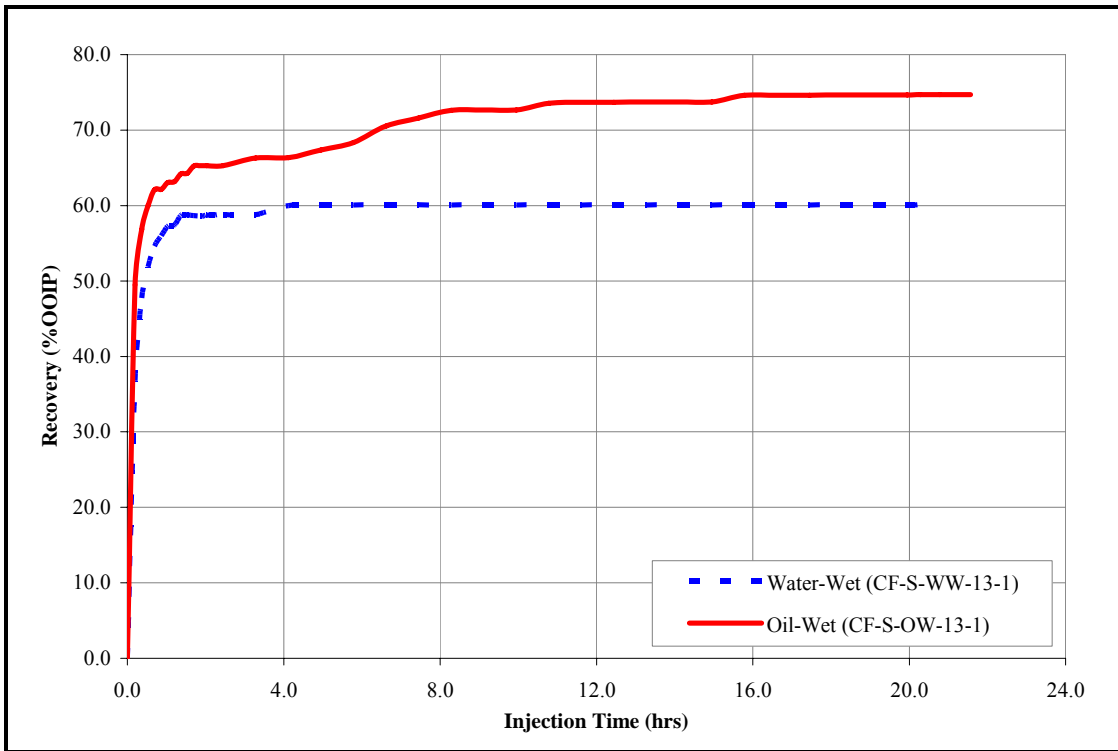


**Figure 4.9:** Effect of the Wettability on the Oil Recovery – Secondary Mode, Constant Rate, 0.13 mm Sand Pack

**Table 4.4:** Model Parameters for the Tertiary Mode Water – Wet Runs

Model Parameters	CP-T-WW-13-3	CP-T-WW-13-4	CP-T-WW-15-1
Gas	N <sub>2</sub>	N <sub>2</sub>	N <sub>2</sub>
P (psig)	4	4	4
Rate (cc/min)	N/A	N/A	N/A
D <sub>g</sub> (mm)	0.13	0.13	0.13
<b>INITIAL CONDITIONS</b>			
Porosity $\phi$ (%)	37.4	36.8	38.7
OOIP (cc)	381.4	390.5	400.7
<b>WATER FLOOD</b>			
Water Flood Recovery (%OOIP)	55.5	56.5	63.7
S <sub>or</sub> (%)	31.4	32.0	26.0
Post-WF S <sub>w</sub> (%)	68.6	68.0	74.0
<b>GAS INJECTION</b>			
k (Darcy)	5.4	5.1	3.9
S <sub>wr</sub> (%)	19.5	16.3	16.7
Recovery (% ROIP)	59.2	44.0	54.2
Recovery (% OOIP)	26.4	19.2	19.7
Total Recovery (%OOIP)	81.9	75.7	83.4

The reason for this is probably a departure from normal procedure for the packing of the physical model. After the treatment of the 0.15 mm glass beads with DMDCS, the surface changed markedly by displaying a tendency to stick together, making it quite difficult to use a funnel to pour them into the model. The model was filled by introducing the glass beads into the cavity by hand-packing prior to assembly of the physical model along. This resulted in relatively tighter packing and, therefore, decreased porosity and permeability resulting in a decrease in oil recovery compared with the looser packed 0.13 mm porous media.

**The wettability of the porous medium:**

The positive influence of the alteration of wettability on the GAGD performance can again be seen in the tertiary mode results. For the reasons listed above, the experimental runs using the 0.15 mm glass beads showed a lower total recovery (%OOIP). This is evident when comparing the results in Table 4.5.

However, when comparing the recovery results of the gas injection it can be seen that the GAGD process was more effective using the oil-wet glass beads: there was an average increase of 12.5 %OOIP in the oil recovery (see Figure 4.11).

The incremental recovery of the oil-wet tertiary mode experiments over the water-wet corresponding cases is included in Table 4.6 which summarizes the effect of wettability on GAGD performance.

**Table 4.5:** Model Parameters for the Tertiary Mode Oil – Wet Runs

Model Parameters	CF-T-OW-13-2	CP-T-OW-15-1	CP-T-OW-15-2	CP-T-OW-13-1	CP-T-OW-13-2
Gas	N <sub>2</sub>	N <sub>2</sub>	N <sub>2</sub>	N <sub>2</sub>	N <sub>2</sub>
P (psig)	N/A	4	4	4	4
Rate (cc/min)	300	N/A	N/A	N/A	N/A
D <sub>g</sub> (mm)	0.13	0.15	0.15	0.13	0.13
<b>INITIAL CONDITIONS</b>					
Porosity $\phi$ (%)	39.8	31.5	32.9	36.2	39.1
OOIP (cc)	450.5	336.8	387.4	400.7	410.5
<b>WATERFLOOD</b>					
Water Flood Recovery (%OOIP)	47.6	40.3	48.9	50.4	46.4
S <sub>or</sub> (%)	41.0	44.2	41.6	38.0	38.9
Post-WF S <sub>w</sub> (%)	59.0	55.8	58.4	62.0	61.1
<b>GAS INJECTION</b>					
k (Darcy)	5.5	3.5	4.2	4.1	4.1
S <sub>wr</sub> (%)	15.3	18.5	17.4	14.1	14.1
N <sub>B</sub>	6.8E-06	5.5E-06	6.3E-06	5.5E-06	8.1E-06
N <sub>C</sub>	1.8E-06	1.2E-06	9.2E-07	8.2E-07	6.2E-07
N <sub>G</sub>	0.4	4.7	6.9	6.8	13.0
Recovery (% ROIP)	62.8	58.1	58.1	62.9	74.0
Recovery (% OOIP)	32.9	34.7	29.7	31.2	39.7
Total Recovery (%OOIP)	80.5	75.0	78.6	81.6	86.1

### 4.3 The Experiments Simulating a Fracture

#### 4.3.1 The Results

The last series of experiments was focused on studying the effect of a vertical fracture in the porous medium on the GAGD performance, taking into account the effect of the wettability of the porous medium. The fracture simulations were done by placing a mesh

box inside the physical model prior to packing the bead or sand pack and conducting the gas displacement experiments. The results are summarized in Table 4.7.

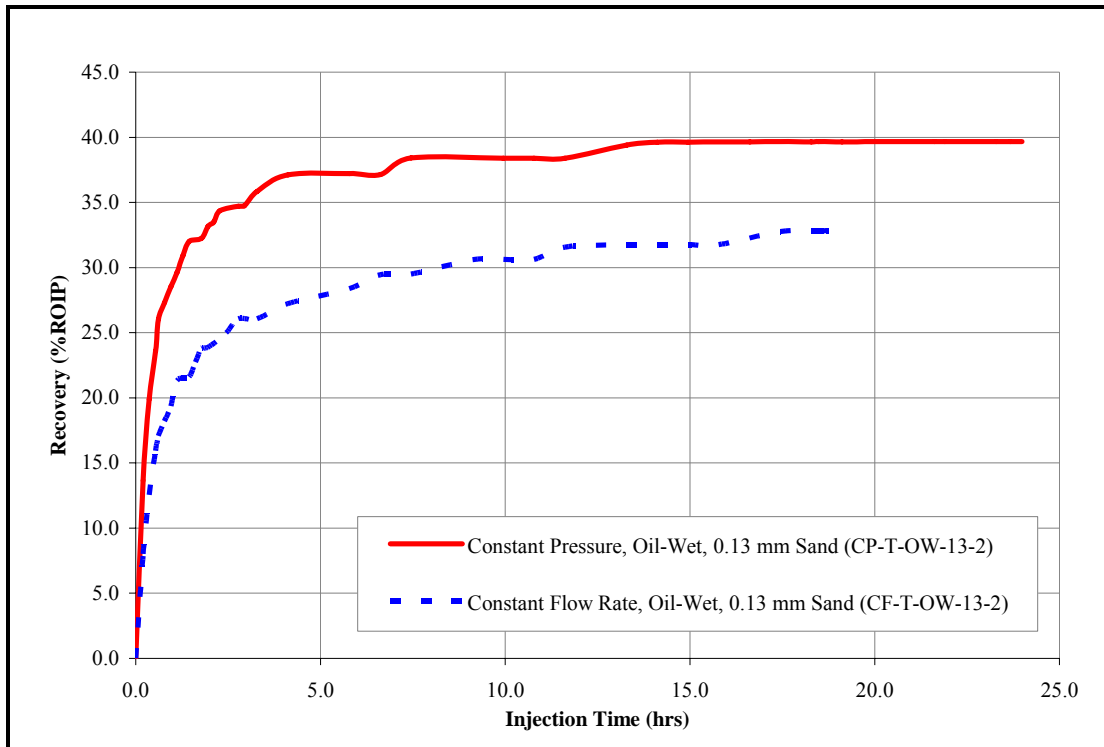


**Figure 4.10:** Effect of Gas Injection Method on the Oil Recovery – Tertiary Mode Runs

#### 4.3.2 Discussion of the Results

The results of the fracture simulation experiments can be compared to the non-fractured experiments with regard to the effect of the presence of a fracture on GAGD performance and within the series the discussion of the results can be grouped according to the wettability of the porous medium and the average grain size of the bead or sand pack.

##### (a) Comparison with the non-fractured experiments:

The presence of the vertical fracture in the physical model seems to improve the GAGD recovery as is evident from Figure 4.13. The incremental effects of the fracture on the oil recovery are summarized in Table 4.8. The average incremental increase in oil recovery is 7.9 %OOIP. It is thought that the increase in oil recovery is caused by the presence of the fracture, which acts as a low resistance conduit for flow of the oil, thus enhancing the oil recovery by gas injection. The injected gas pushes the oil into the fracture giving the

oil an easier way to drain out of the porous medium. This is shown pictorially in Figure 4.14, where the white arrows point to the matrix areas in the model from which the oil was driven to the nearby fracture.

**Table 4.6:** Summary of Incremental Effect of the Wettability on the Oil Recovery

Description of Experiment	Oil Recovery (%OOIP)	
	Actual	Incremental over Water-Wet
CF secondary 0.13 mm	74.7	14.6
CP secondary 0.13 mm	75.9	9.2
CP secondary 0.15 mm	81.1	8.4
CP tertiary 0.13 mm	74.0*	14.8*
CP tertiary 0.15 mm	58.1*	3.9*

\*Note: Oil recovery in %ROIP.

However, when we compare the water-wet fractured model runs using the 0.15 mm glass beads with their non-fractured counterpart, it is evident that both of the fractured runs performed worse than the non-fractured run (see Figure 4.15). This is probably caused by an incomplete oil flood: during the initial displacement of water with n-decane from the top to the bottom, it could be noticed that there consistently were parts of the porous medium that were being bypassed by the n-decane (see Figure 4.16). It is believed that this is caused by the inherent higher permeability due to the use of a larger grain size creating easier flow paths to the fracture. This problem could not be resolved even when the oil flood was extended longer than normal (the oil flood was stopped in both cases when no more oil had been produced for a period longer than 4 hours).

By examining the results of the oil-wet fractured runs and comparing them with the experiments without a fracture, it can be seen in all runs that the fractured cases outperform the non-fractured ones (see Figures 4.17 and 4.18). On average, the incremental oil recovery was 6.7 %OOIP for the experiments using the 0.13 mm silica sand.

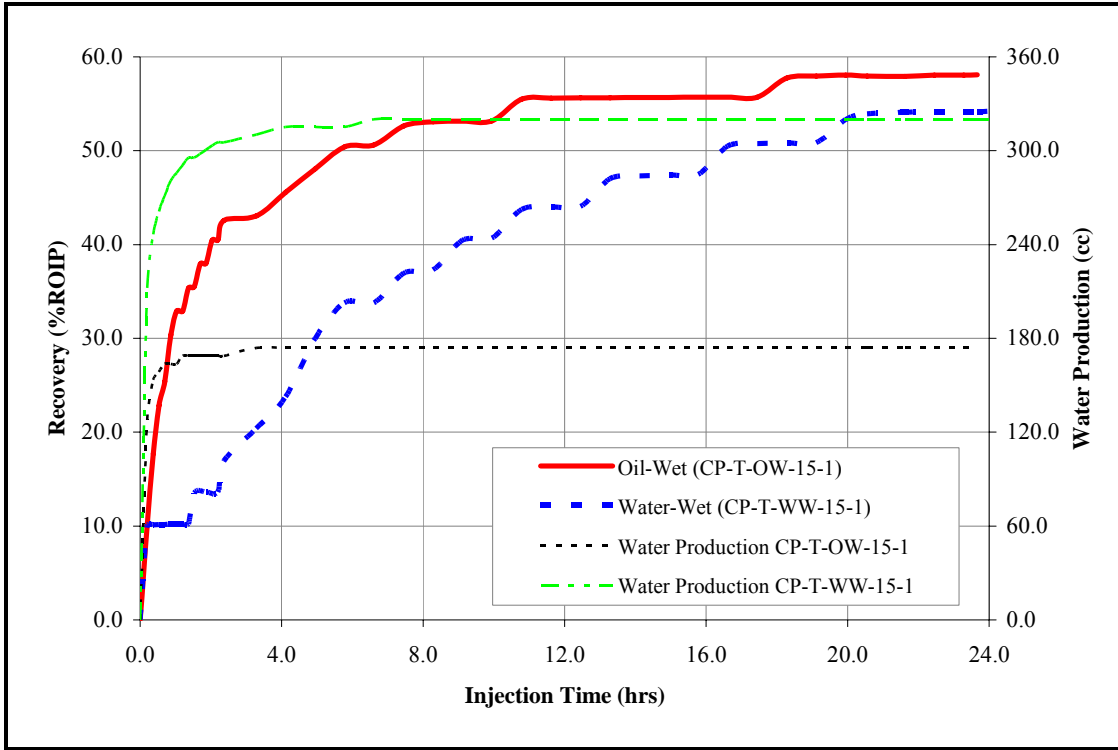


**Figure 4.11:** Effect of the Wettability on the Oil Recovery – Tertiary Mode, 0.15 mm Glass Bead Pack

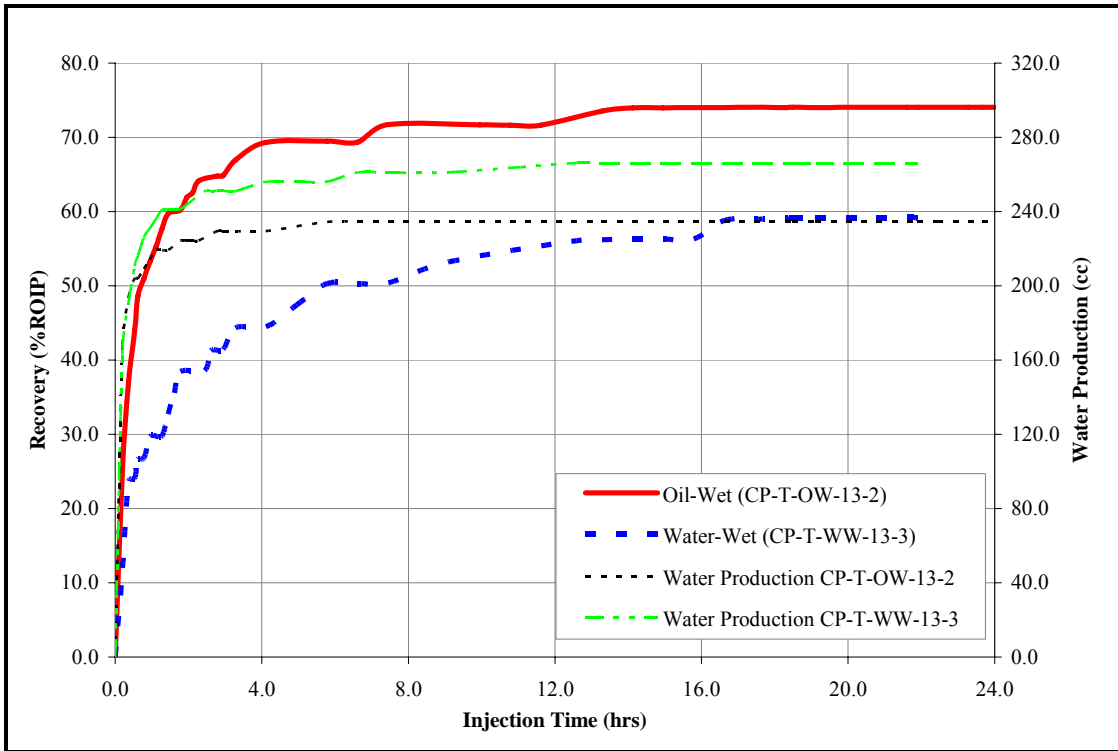


**Figure 4.12:** Effect of the Wettability on the Oil Recovery – Tertiary Mode, 0.13 mm Sand Pack

**Table 4.7:** Model Parameters for the Fracture Simulation Runs

Model Parameters	CP-S- WW-13- 1-F	CP-S- WW-13- 2-F	CP-S- OW-13- 1-F	CP-S- OW-13- 2-F	CP-S- WW-15- 1-F	CP-S- WW-15- 2-F	CP-S- OW-15- 1-F
Gas	N <sub>2</sub>	N <sub>2</sub>	N <sub>2</sub>	N <sub>2</sub>	N <sub>2</sub>	N <sub>2</sub>	N <sub>2</sub>
Wettability State	Water-wet	Water-wet	Oil-wet	Oil-wet	Water-wet	Water-wet	Oil-wet
P (psig)	4	4	4	4	4	4	4
Rate (cc/min)	N/A	N/A	N/A	N/A	N/A	N/A	N/A
D <sub>g</sub> (mm)	0.13	0.13	0.13	0.13	0.15	0.15	0.15
<b>INITIAL CONDITIONS</b>							
Pore Volume (cc)	565.0	587.5	545.0	587.8	584.0	592.0	547.0
Oil Flood Water (cc)	323.7	363.7	463.7	380.2	303.7	338.7	468.7
OOIP (cc)	323.7	363.7	463.7	380.2	303.7	338.7	468.7
Porosity $\phi$ (%)	39.1	40.7	37.7	40.7	40.4	41.0	37.9
S <sub>wc</sub> (%)	42.7	38.1	14.9	35.3	48.0	42.8	14.3
S <sub>oi</sub> (%)	57.3	61.9	85.1	64.7	52.0	57.2	85.7
<b>GAS INJECTION</b>							
k (Darcy)	N/A	N/A	N/A	N/A	N/A	N/A	N/A
N <sub>B</sub>	N/A	N/A	N/A	N/A	N/A	N/A	N/A
N <sub>C</sub>	N/A	N/A	N/A	N/A	N/A	N/A	N/A
N <sub>G</sub>	N/A	N/A	N/A	N/A	N/A	N/A	N/A
Recovery (% OOIP)	74.6	71.2	54.7	82.5	68.6	72.0	91.9

**Table 4.8:** Summary of the Incremental Effect of the Fracture on the Oil Recovery

Description of Experiment	Oil Recovery (%OOIP)	
	Actual	Incremental over Non-Fractured
CP secondary fractured water-wet 0.13 mm	72.9	6.2
CP secondary fractured oil-wet 0.13 mm	82.5	6.7
CP secondary fractured oil-wet 0.15 mm	91.9	10.8

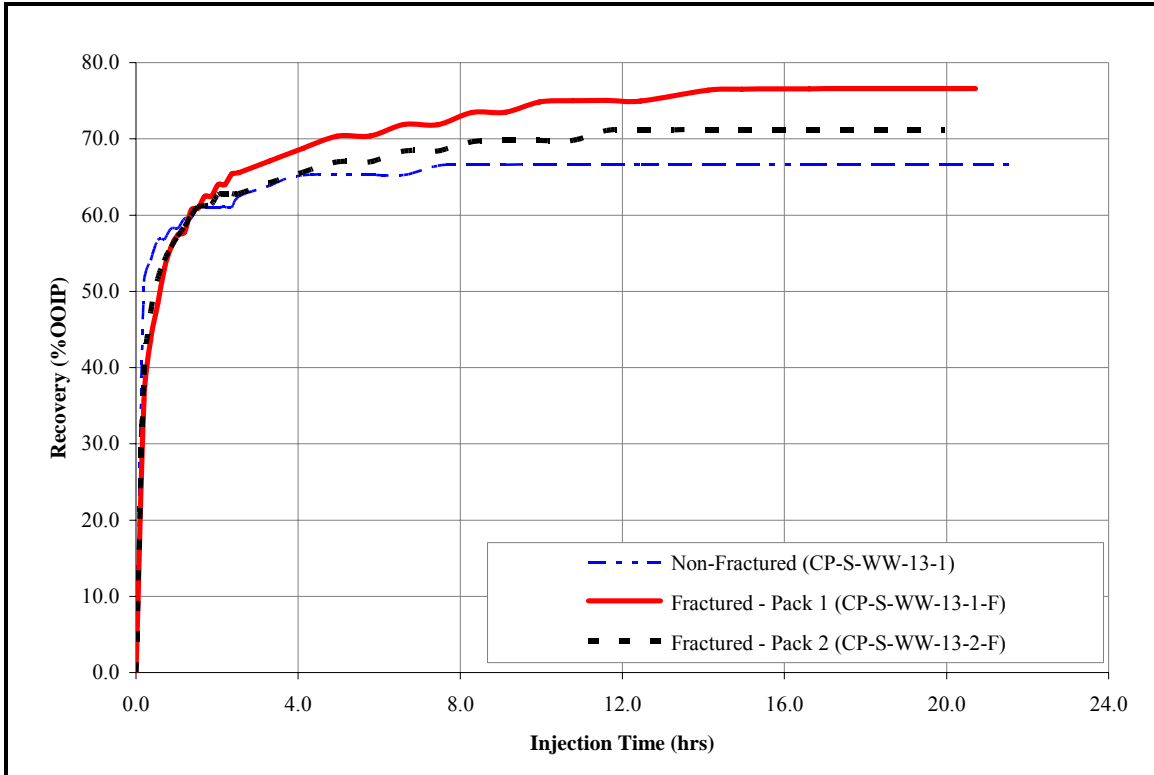


**Figure 4.13:** Effect of a Vertical Fracture on the Oil Recovery – Water-Wet Case, 0.13 mm Sand Pack

For the 0.15 mm glass bead packs, the average increase in the oil recovery was 10.8 %OOIP. The problem of certain parts of the porous medium being bypassed was not encountered in the experiments using the oil-wet particles because of the preferential spreading of the oil on the pore surfaces. In this discussion, CP-S-OW-13-1-F was not taken into consideration because it was just a trial run to test the integrity of the fracture.

**(b) The wettability of the porous medium:**

By comparing the results of the various fractured experiments, it is clear that the wettability of the porous medium definitely has an effect on the GAGD performance in conjunction with the presence of the fracture.

All of the oil-wet experiments showed an increase in the oil recovery compared to the water-wet fracture runs (see Figures 4.19 & 4.20 and Table 4.9):

- Oil-wet, fractured 0.13 mm silica sand pack: an incremental oil recovery of 9.6 %OOIP on average.
- Oil-wet, fractured 0.15 glass bead pack: an incremental oil production of 21 %OOIP.



**Figure 4.14:** Gas Injection Profile into Water-Wet Fracture Simulation – 0.13 mm

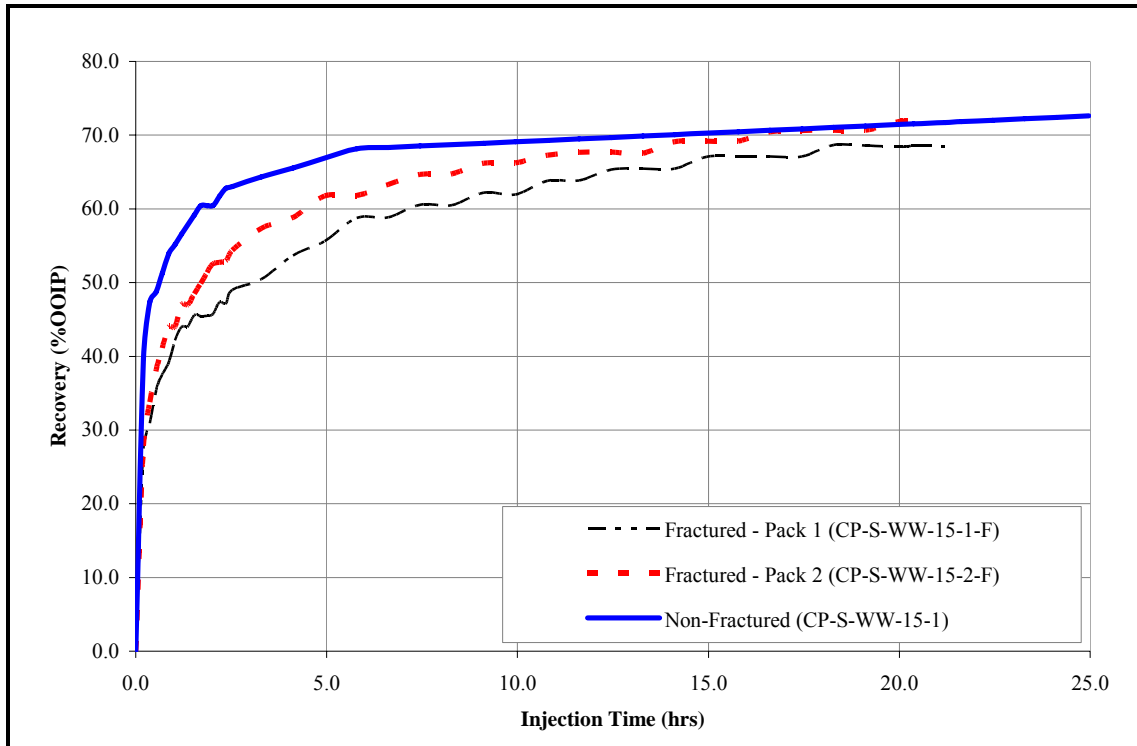


**Figure 4.15:** Effect of a Vertical Fracture on the Oil Recovery – Water-Wet Case, 0.15 mm Glass Bead Pack

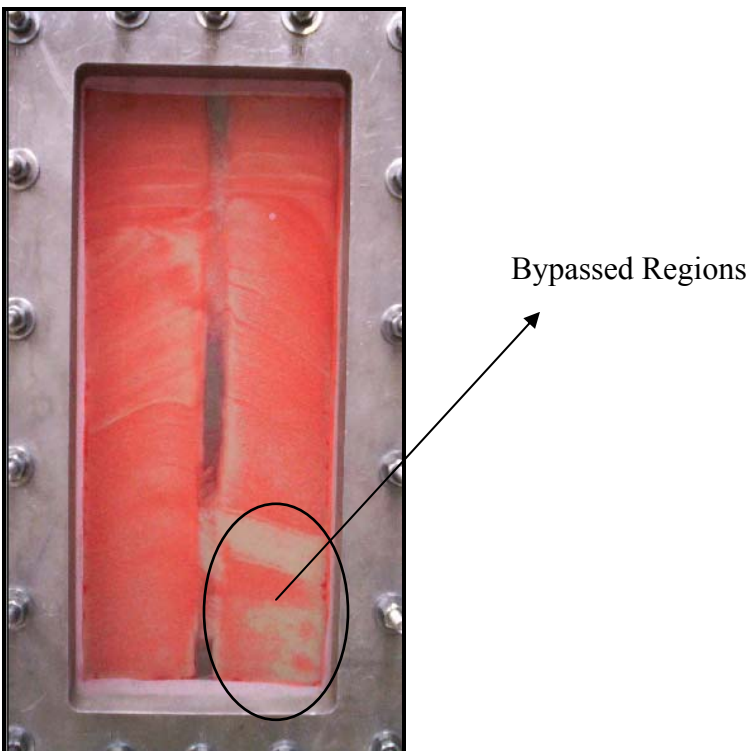


**Figure 4.16:** Regions Bypassed by N-Decane Flood in Fracture Simulation – Water-Wet, 0.15 mm

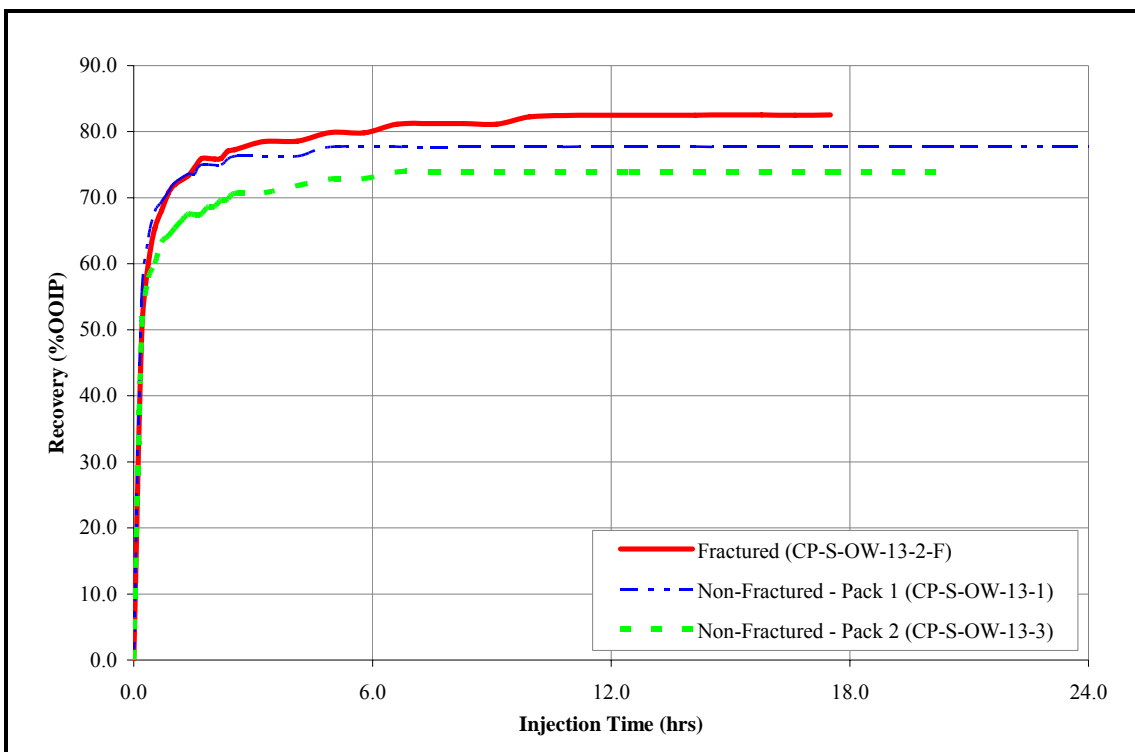


**Figure 4.17:** Effect of a Vertical Fracture on the Oil Recovery – Oil-Wet Case, 0.13 mm Sand Pack

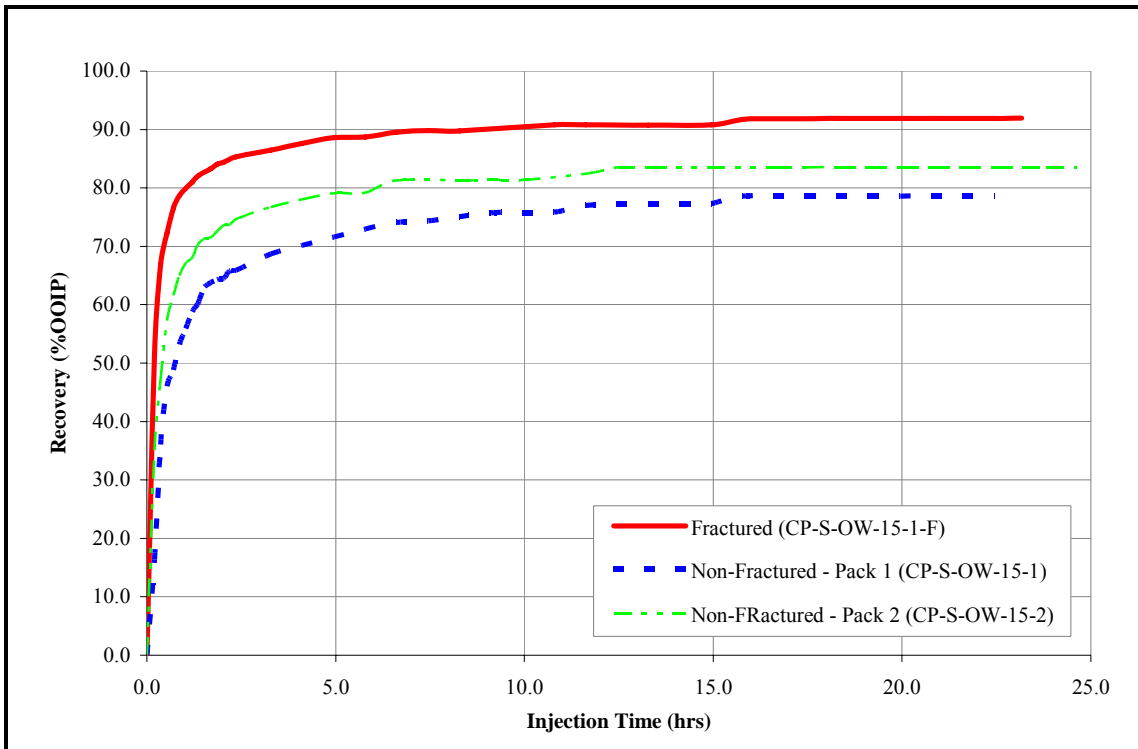


**Figure 4.18:** Effect of a Vertical Fracture on the Oil Recovery – Oil-Wet Case, 0.15 mm Glass Bead Pack

**Table 4.9:** Summary of the Incremental Effect of the Wettability on the Fractured Runs

Description of Experiment	Oil Recovery (%OOIP)	
	Actual	Incremental over Water- Wet
CP secondary fractured 0.13 mm	82.5	9.6
CP secondary fractured 0.15 mm	91.9	21.6

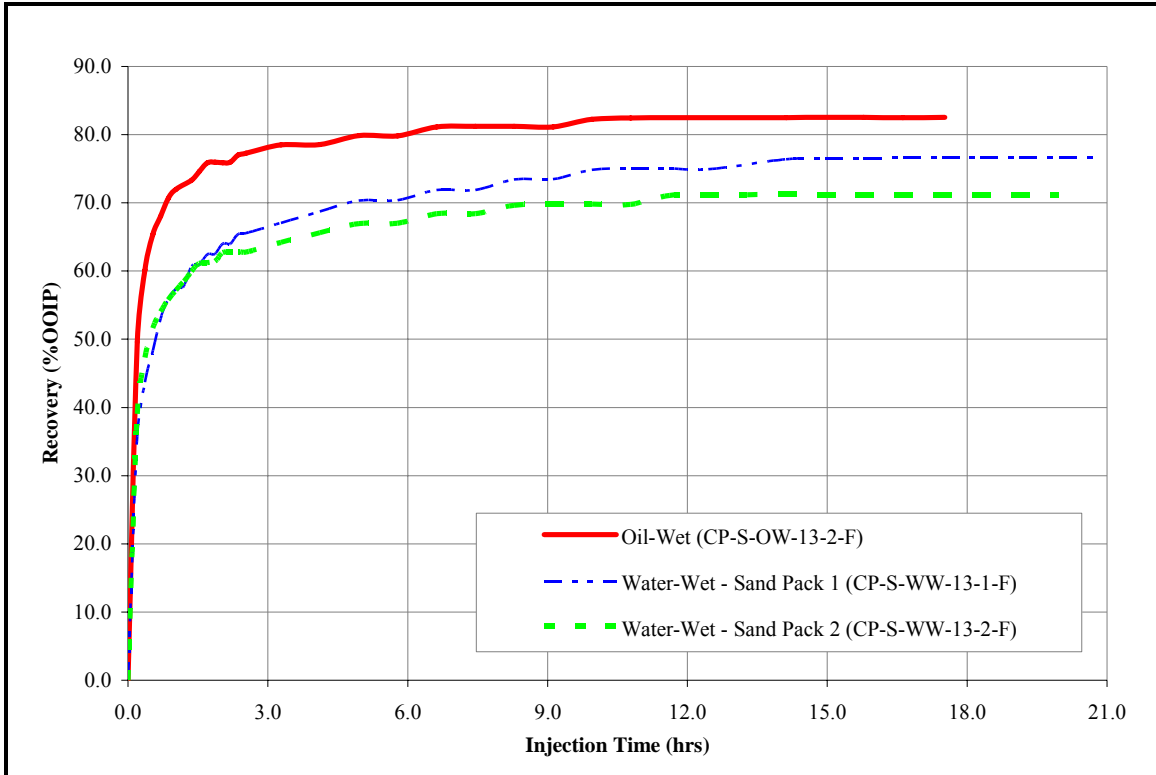


**Figure 4.19:** Effect of the Wettability on Fractured Runs – 0.13 mm Sand Pack

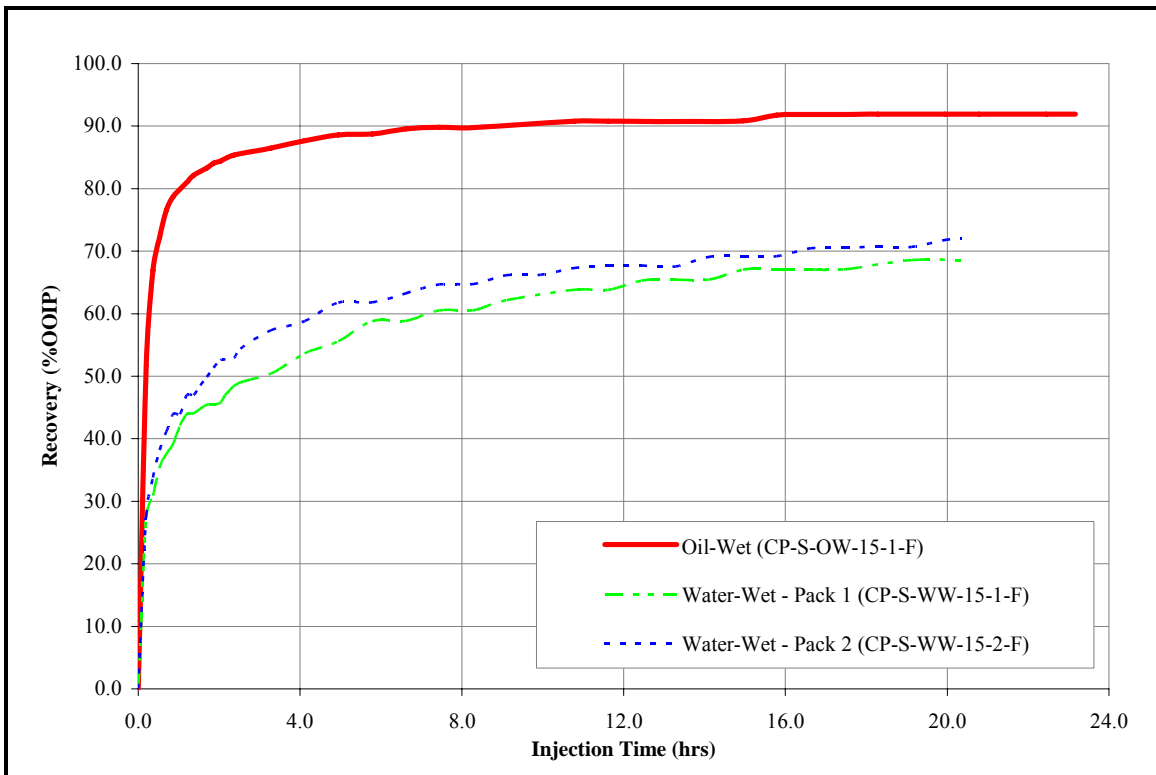


**Figure 4.20:** Effect of the Wettability on Fractured Runs – 0.15 mm Glass Bead Pack

**(c) The average grain size of the porous medium:**

It was expected that the experiments using the larger grain size would show the same increase in oil recovery as was the case with the non-fractured runs. However, this only happened with the oil-wet runs. The water-wet runs experienced problems with bypassed regions during the oil flood using the larger grain size due to the reasons previously mentioned, thus leading to a seemingly poorer performance of the gas displacement (see Figure 4.21). The oil-wet experiment using the larger grain size did follow the expected increase in oil recovery because of the increase in permeability (see Figure 4.22).

**4.4 The Dimensionless Groups**

Although the effect of the dimensionless groups on the GAGD performance was not a main focus in the study, their value was calculated for the various gas displacement experiments for comparison with the results by Sharma (Table 4.10).

In the literature review section the following dimensionless groups were defined:

1. The Bond number,  $N_B = \frac{\Delta\rho_{og} g Z R_a}{2\sigma_{go}}$ , a dimensionless group that is a measure of

the relative strength of gravity versus capillary forces.  $Z$  is the average position of the gas interface and  $R_a$  represents the average pore throat radius, both a function of the absolute permeability and the porosity of the porous medium. The Bond number can thus be rewritten as:

$$N_B = \frac{\Delta\rho g \frac{K}{\phi}}{\sigma_{go}} \text{-----} (9)$$

In this equation,  $K$  is the absolute permeability and  $\phi$  is the porosity of the porous medium.

2. The capillary number,  $N_C = \frac{v \mu}{\sigma \cos\theta}$ , is a measure of the relative strength of the viscous to the capillary forces.

Shook et al. (1992) have defined a new scaling group that appears to be a combination of the Bond number and the capillary number, relating the gravity forces to the viscous forces:

$$N_g = \frac{k_x \lambda_{r2}^o \Delta \rho g \cos \alpha H}{u_T L} \text{-----} (10a)$$

which Sharma (2005) rewrote for 2-D vertical flow as:

$$N_G = \frac{\Delta \rho g \frac{K}{\phi}}{\mu v} \text{-----} (10b)$$

where:

- $\Delta \rho$  is the density contrast between the gas phase and the oleic phase;
- $g$  is the gravitational constant;
- $K$  is the absolute permeability of the porous medium;
- $\phi$  is the porosity of the porous medium;
- $\mu$  is the viscosity of the oleic phase;
- $v$  is the Darcy velocity.

Shook et al. (1992) called this group the buoyancy group because it depends on a density difference rather than just a density, while Sharma (2005) referred to it as the gravity number. The latter term shall be used in this study.

#### 4.4.1 The Bond Number

The relation between the Bond number and the oil recovery is plotted in Figure 4.23. The Bond number is a relative measure of the gravity forces to the capillary forces and as such it can be expected that the recovery will be higher when the flow of fluids is gravity-dominated. This occurs at higher values of the Bond number. However, looking at Figure 4.23, it is obvious that this is not the case for the oil-wet secondary runs compared to the water-wet secondary mode runs conducted by Sharma (2005). The experiments conducted by Sharma show the expected trend of increasing recovery with higher values

for the Bond number. The results from this study seem to indicate that higher oil recoveries can be achieved in oil-wet cases even at low Bond numbers, probably because of the continuity of the oil film on the pore surfaces aiding low residual oil saturations. This can also be seen when the oil-wet tertiary runs expressed in %ROIP are examined (also in Figure 4.23). More definite conclusions cannot be derived because of the narrow range of the Bond number of the experiments conducted in this study.

#### **4.4.2 The Capillary Number**

When comparing the secondary mode experimental results from this study with those obtained by Sharma (2005) (see Figure 4.24), it is evident that the current results seem to follow a similar trend to the latter ones, as depicted in Figure 4.25.

Upon examination of the equation used to calculate the capillary number, it seems obvious that the limiting factor is the Darcy velocity, which is proportional to the injection rate. This is a valid statement when all other parameters are kept the same, such as porous media fluids and injected gas. Although it was a concern that there would have been problems with the injected gas bypassing some oil at higher capillary numbers, it is evident from the results that this was not the case. The same is true for the experiments conducted by Sharma (2005), which leads the author to believe that the experiments were conducted under stable conditions.

#### **4.4.3 Statistical Analysis of the Results**

Using the Statistical Analysis Software (SAS) package, a multiple regression analysis was performed on the experimental results. These results are shown in Figures 4.26 and 4.27 and include the  $\pm 10\%$  - error bands. From the figures it is evident that although the regression model does not fit the experimental data well, only 10% of the secondary mode results lie outside of the  $\pm 10\%$  - error region. However, two-thirds of the tertiary mode experiments results fall outside of the  $\pm 10\%$  - error region. In the figures, the equation for the multiple regression models and the respective  $R^2$ -values are included.

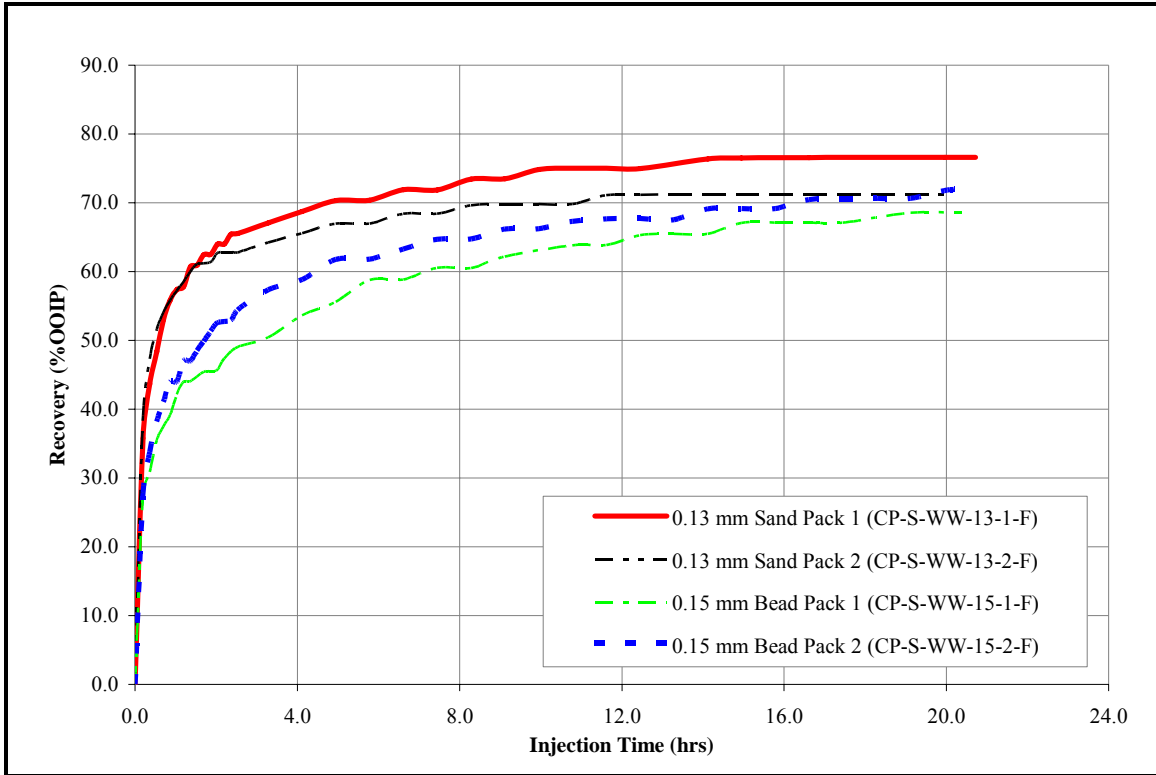


**Figure 4.21:** Effect of Grain Size on Recovery in Fractured Model – Water-Wet Runs

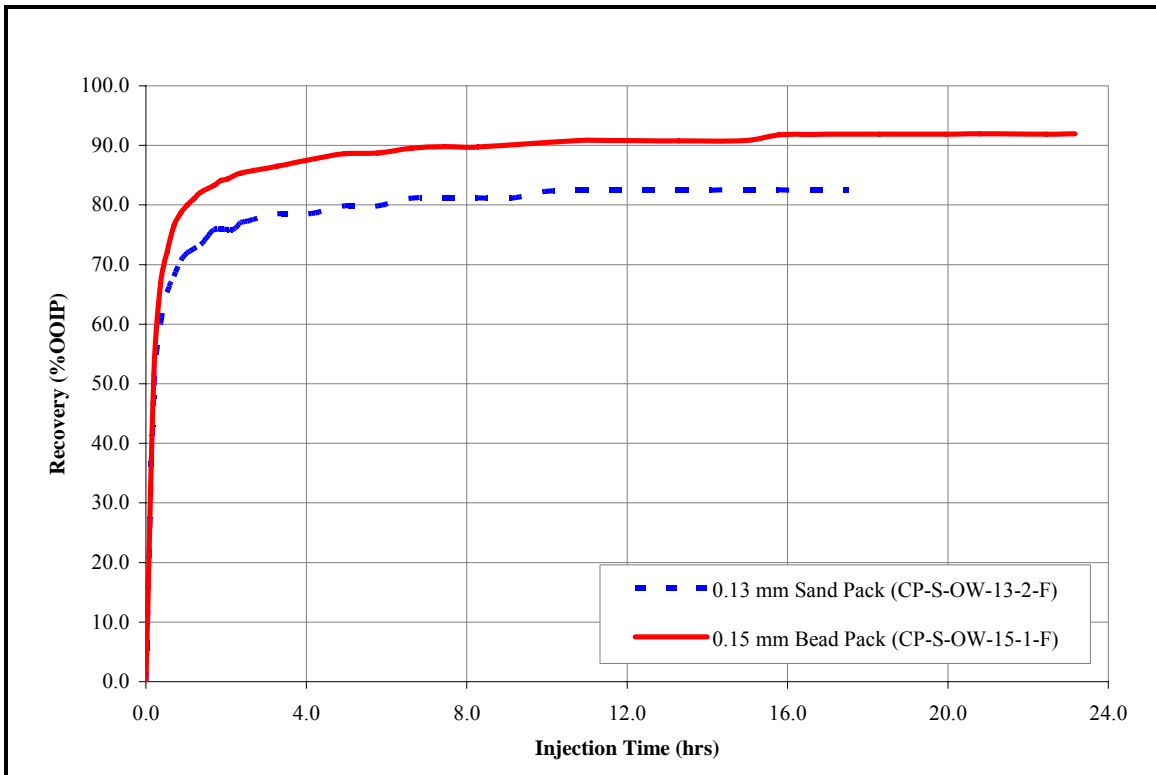


**Figure 4.22:** Effect of Grain Size on Recovery in Fractured Model – Oil-Wet Runs

**Table 4.10:** Experimental GAGD Results of Sharma (2005) – Secondary Mode

Experiment Number	Grain Size (mm)	Gas Flow Rate (cc/min)	Bond Number ( $N_B$ )	Capillary Number ( $N_C$ )	Gravity Number ( $N_G$ )	Oil Recovery (%IOIP)
CP1	0.5	N/A	4.00E-04	1.62E-08	2.47E+04	79.4
CP2	0.5	N/A	4.10E-04	1.95E-08	2.10E+04	78.3
CR1	0.5	20	3.50E-04	5.36E-08	6.53E+03	73.0
CR2	0.15	20	3.60E-05	5.36E-08	6.72E+02	62.0
CR3	0.15	20	3.50E-05	6.43E-08	5.44E+02	59.0
CR4	0.15	20	7.10E-06	6.43E-08	1.10E+02	54.4
CR5	0.15	20	3.00E-05	1.33E-07	2.25E+02	67.0
CR6	0.15	5	3.10E-05	1.60E-08	1.94E+03	49.0
CR7	0.15	400	3.10E-05	1.28E-06	2.42E+01	72.0
CR8	0.15	200	3.21E-05	6.43E-07	4.99E+01	69.5
CR9	0.15	300	3.50E-05	9.64E-07	3.63E+01	70.9

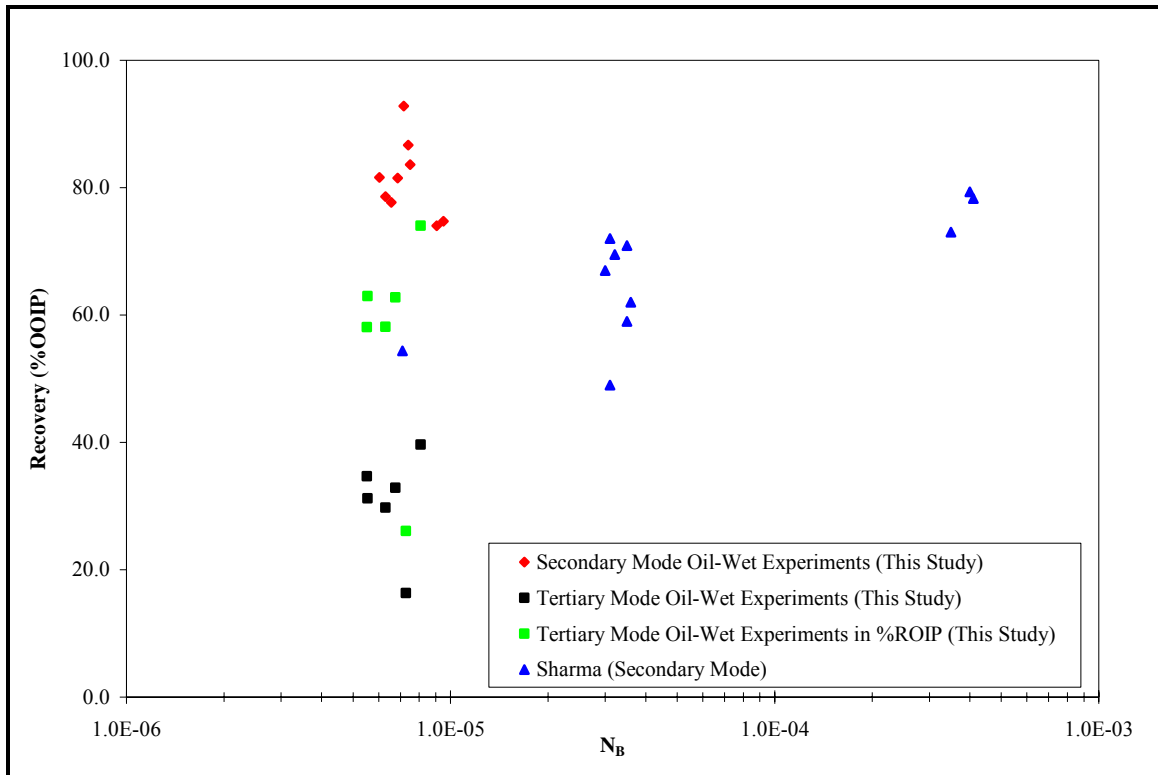


**Figure 4.23:** The Relation between the Bond Number and Oil Recovery

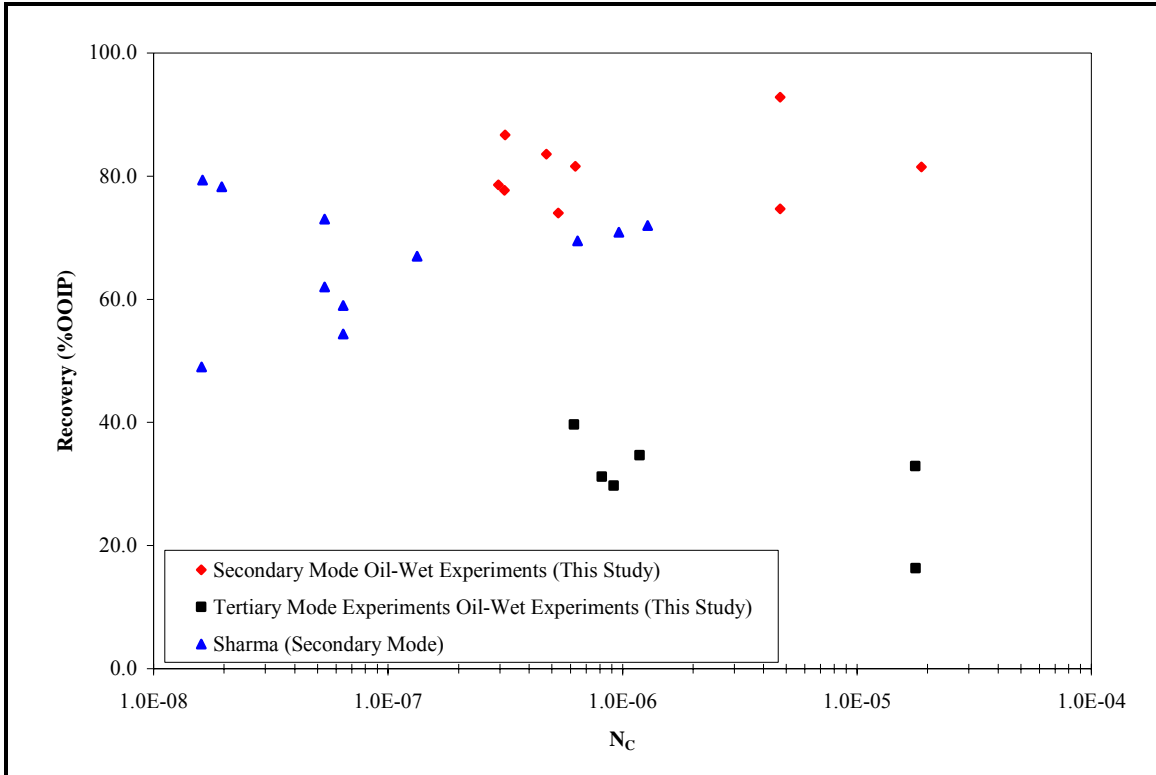


**Figure 4.24:** The Relation between the Capillary Number and Oil Recovery

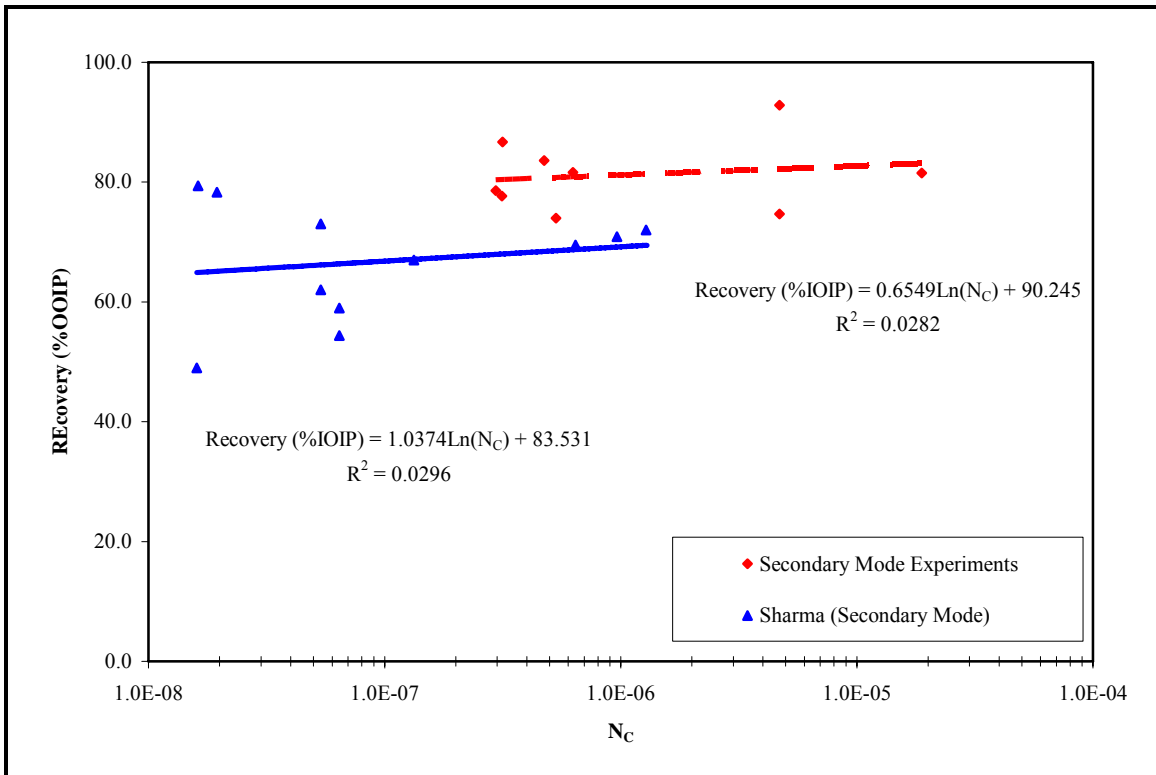


**Figure 4.25:** Similarities between the Capillary Number Trends

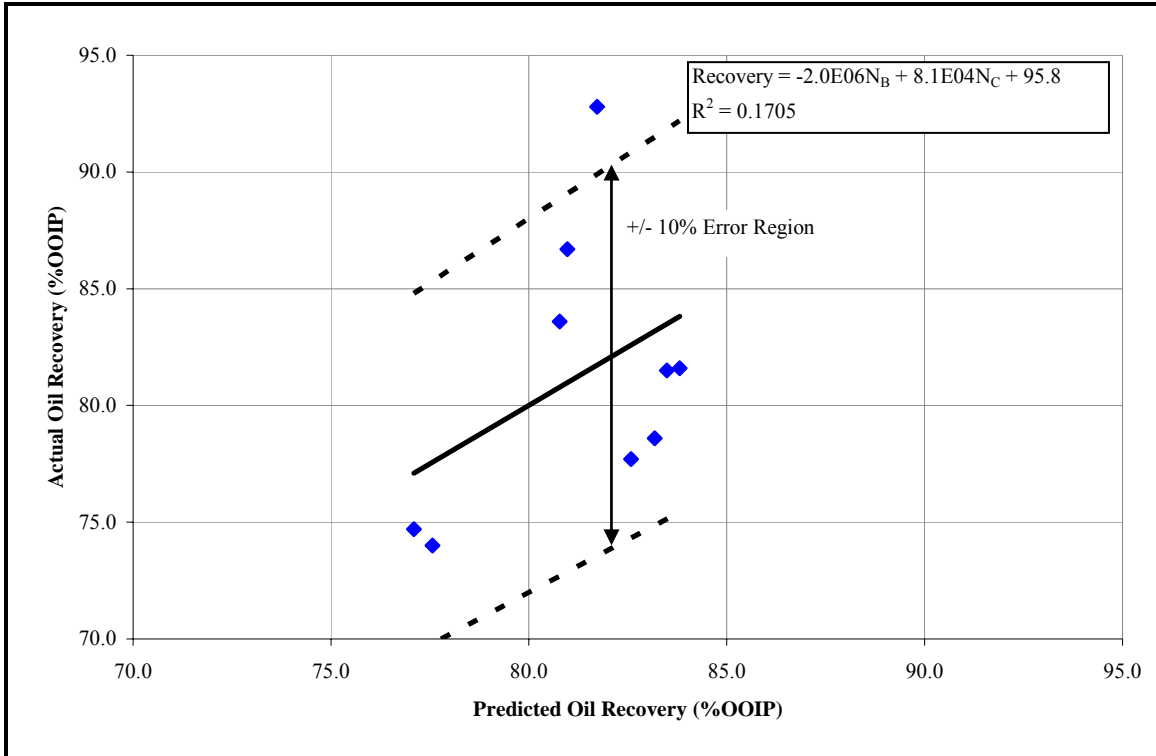


**Figure 4.26:** Multiple Regression Analysis Results for the Secondary Mode Experiments

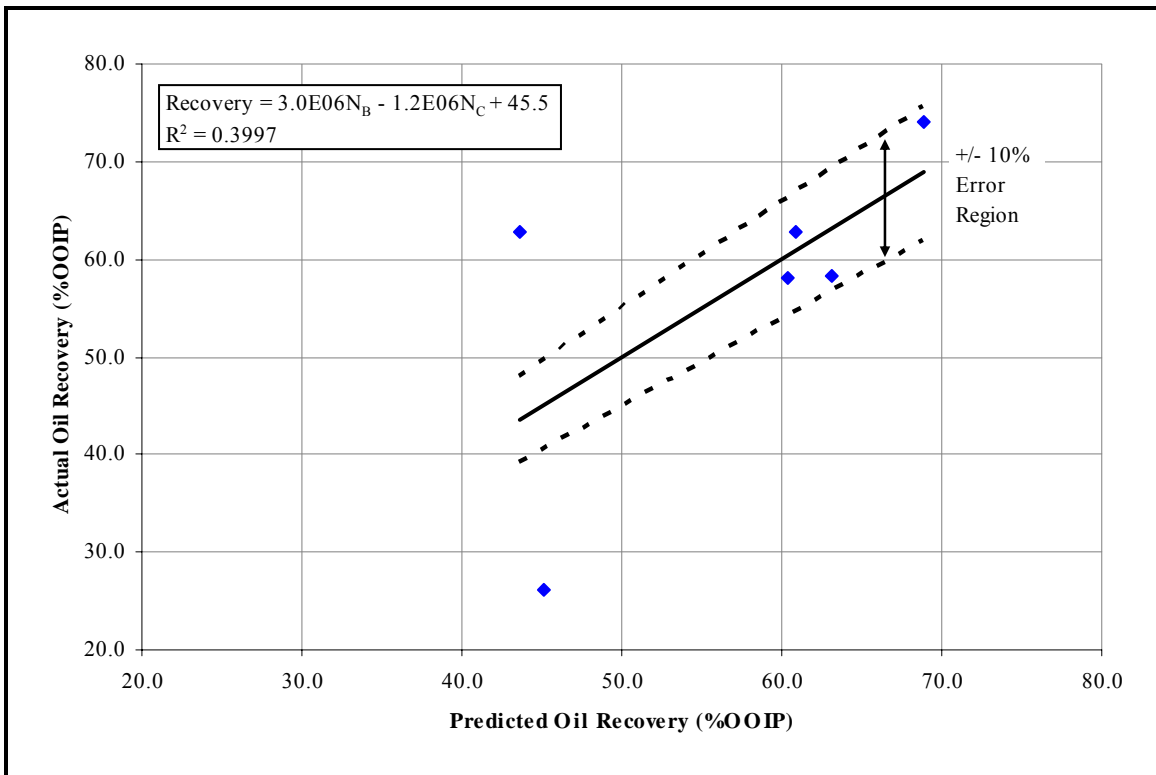


**Figure 4.27:** Multiple Regression Analysis Results for the Tertiary Mode Experiments

## CHAPTER 5

### CONCLUSIONS AND RECOMMENDATIONS

#### 5.1 Summary of Findings and Conclusions

In this study, physical model experiments were conducted to study the effects of the wettability of the porous medium and the presence of a fracture on the performance of the GAGD process. The physical model used was a simple Hele-Shaw type model incorporating either soda glass beads or silica sand as the porous media and n-decane and deionized water as the fluids in the porous medium. The glass beads or silica sand were rendered oil-wet by a treatment with the organosilane dimethyldichlorosilane. The gas displacement experiments were conducted using nitrogen or carbon dioxide under constant pressure or under constant mass flow rate. The gas displacement strategy was also varied resulting in a series of experiments in the secondary mode and one in the tertiary mode (i.e. the gas displacement followed a water flood). The presence of a vertical fracture was simulated by placing a mesh box in the model prior to packing the bead or sand pack and conducting gas displacement experiments under the conditions described above.

The important conclusions that can be drawn from the experiments conducted in the study are:

1. The wettability affects the performance of the GAGD process – on average, the use of an oil-wet porous medium improved the performance of the GAGD process by an increase of 12.7 % in the recovery of the original oil in place.
2. The presence of a vertical fracture in the porous medium improves the performance of the GAGD process. The average incremental production because of the presence of the vertical fracture in the physical model experiments was 7.8 % (%OOIP).
3. The type of gas injected affects the performance of the GAGD process when using an oil-wet porous medium in the physical model experiments: an increase of 10.9 %OOIP was seen when using CO<sub>2</sub>. Sharma (2005) had already shown that the type of gas does not affect the GAGD performance when the experiments are conducted in a water-wet porous medium.

4. The constant pressure gas displacement of the oil in the experiments results in a slightly higher recovery (2.6-3.0 %OOIP) compared to the constant rate displacement experiments.
5. The Bond number seems to have less of an influence in oil-wet porous media than in water-wet media owing to the fact that the continuity of the oil film overcomes any adverse effects of the capillary forces.
6. The oil recovery improves as the capillary number increases and the observed logarithmic relationship between them is very similar to the one obtained by Sharma (2005).

## **5.2 Recommendations for Future Work**

In the present study the wettability state of the porous medium was quantified using the Amott method. An alternative to this method would be the determination of the wettability state through the measurement of the contact angle of both treated and untreated glass slides.

As Sharma (2005) already suggested:

Scaled experiments using horizontal wells are also recommended to study the productivity of horizontal wells during the GAGD process, and also to develop a working fully scaled experimental model to compare GAGD with other production schemes. (p. 81)

The above mentioned recommendation is even more valid since the applicability of the GAGD process in oil-wet porous media has been demonstrated by the results from this study.

To increase the scope of its applicability, the GAGD process should also be tested using varying configurations of the injection wells and the producers, as well as the fracture orientation and frequency of occurrence.

## REFERENCES

1. Anderson, W.G. (1986). Wettability Literature Survey – Part 2: Wettability Measurement. *SPE Paper 13933*, pp. 1246-62.
2. Catalan, L.J.J., Dullien, F.A.L. & Chatzis, I. (1994). The Effects of Wettability and Heterogeneities on the Recovery of Waterflood Residual Oil With Low Pressure Inert Gas Injection Assisted by Gravity Drainage. *SPE Paper 23596*, pp. 140-149.
3. Caudle, B.H. & Dyes, A.B. (1959). Improving Miscible Displacement by Gas-Water Injection. *Transactions of AIME, Volume 213*, pp. 281-284.
4. Christensen, J.R., Stenby, E.H. & Skauge, A. (1998). Review of WAG Field Experience. *Paper SPE 39883, presented at the SPE International Petroleum Conference and Exhibition, Villahermose, Mexico, 3-5 March 1998*.
5. Darvish, G.R., Lindeberg, E., Kleppe, J. & Torsæter, O. (not dated). *Numerical Simulations for Designing Oil/CO<sub>2</sub> Gravity-Drainage Laboratory Experiments of a Naturally Fractured Reservoir*. Retrieved 2/19/06 from [http://www.iku.sintef.no/projects/IK54525400/reports/320\\_Reza\\_revised.pdf](http://www.iku.sintef.no/projects/IK54525400/reports/320_Reza_revised.pdf)
6. Grattoni, C.A., Jing, X.D., & Dawe, R.A. (2001). Dimensionless Groups for Three-Phase Drainage Flow in Porous Media. *Journal of Petroleum Science and Engineering, Volume 29*, pp. 53-65.
7. Hair, M.L. (1986). Silica Surfaces. In Leyden, D.E. (Ed.), *Silanes, Surfaces and Interfaces* (pp. 25-41). New York, USA: Gordon and Breach Science Publishers.
8. Johnson, E.F., Bossler, D.P., & Naumann, V.O. (1957). Calculation of Relative Permeability from Displacement Experiments. *SPE Paper 1023-G*, pp. 370-372.
9. Lake, L.W. (1989). *Enhanced Oil Recovery*. New Jersey: Prentice-Hall Inc.
10. Lake, L.W., Schmidt, R.L., & Venuto, P.B. (1992). A Niche for Enhanced Oil Recovery in the 1990s. *Oilfield Review, January 1992*, pp. 55-61. Retrieved 2/16/06 from [http://www.slb.com/media/services/resources/oilfieldreview/ors92/0192/p55\\_61.pdf](http://www.slb.com/media/services/resources/oilfieldreview/ors92/0192/p55_61.pdf)
11. Lenormand, R., Touboul, E., & Zarcone, C. (1988). Numerical Models and Experiments on Immiscible Displacements in Porous Media. *J. Fluid Mechanics, Volume 189*, pp. 165-187.
12. Li, Y. & Wardlaw, N.C. (1986). The Influence of Wettability and Critical Pore-Throat Size Ratio on Snap-off. *J. Colloid Interface Sci., No. 2*, pp. 461-72.

13. Morrall, S.W., & Leyden, D.E. (1986). Modification of Siliceous Surfaces with Alkoxysilanes from a Nonaqueous Solvent. In Leyden, D.E. (Ed.), *Silanes, Surfaces and Interfaces* (pp. 501-524). New York, USA: Gordon and Breach Science Publishers.
14. Morrow, N.R. (1990). Wettability and Its Effect on Oil Recovery. *SPE Paper 21621*, pp.1476-84.
15. Muskat, M. (1981). *Physical Principles of Oil Production*. Boston, MA: McGraw-Hill Book Company.
16. Naylor, P. & Frørup, M. (1989). Gravity-Stable Nitrogen Displacement of Oil. *SPE Paper 19641*, pp. 155-166.
17. Panda, M.N., & Lake, L.W. (1994). Estimation of Single-Phase Permeability from the Parameters of a Particle-Size Distribution. *AAPG Bulletin*, v. 78, no. 7, pp. 1028-1039.
18. Plueddeman, E.P. (1982). *Silane Coupling Agents*. New York: Plenum Press.
19. Plueddeman, E.P. (1986). Silane Compounds for Silylating Surfaces. In Leyden, D.E. (Ed.), *Silanes, Surfaces and Interfaces* (pp. 1-24). New York, USA: Gordon and Breach Science Publishers.
20. Sharma, A.P. (2005). *Physical Model Experiments of the Gas-Assisted Gravity Drainage Process*. M.S. Thesis, LSU – Craft & Hawkins Department of Petroleum Engineering.
21. Shook, M., Li, D. & Lake, L.W. (1992). Scaling Immiscible Flow through Permeable Media by Inspectional Analysis. *In Situ*, 16(4), pp. 311-49.
22. Tiab, D. & Donaldson, E.C. (1996). *Petrophysics – The Theory and Practice of Measuring Reservoir Rock and Fluid Transport Properties*. Houston, USA: Gulf Publishing Company.
23. Rao, D.N., Ayirala, S.C., Kulkarni, M.M. & Sharma, A.P. (2004). Development of Gas Assisted Gravity Drainage Process for Improved Light Oil Recovery. *Paper SPE 89357*, pp. 1-12.
24. Ren, W., Bentsen, R. & Cunha, L.B. (2004). Pore-Level Observation of Gravity-Assisted Tertiary Gas-Injection Processes. *SPE Paper 88801*, pp. 194-201.
25. Vizika, O. & Lombard, J.-M. (1994). Wettability and Spreading: Two Key Parameters in Oil Recovery with Three-Phase Gravity Drainage. *SPE Paper 28613*, pp. 54-60.

## VITA

Wagirin Ruiz Paidin was born in Paramaribo, Suriname, on March 7, 1977, the son of Wagimin Samben Paidin and Toegijem Trirarbijah Paidin-Resowidjojo. After completing his high school studies at the Algemene Middelbare School, Paramaribo, Suriname, he joined the Department of Mining and Geology of the School of Natural Sciences at the Anton De Kom University of Suriname, and obtained the degree Bachelor of Science in Mining in 2001. He worked as a junior geologist in charge of sampling and borehole logging for the Gold Division of the ALCOA, L.L.C. in Merian Creek, Suriname, from 2001 to 2002. In 2003, he enrolled in the post-graduate diploma course petroleum technology offered through the cooperation of the State Oil Company of Suriname (Staatsolie N.V.), the University of Suriname and the Technical University at Delft. As a result of completing the course at the top of the class he joined the Graduate School of the Louisiana State University, Baton Rouge, U.S.A. in August 2004. The degree of Master of Science in Petroleum Engineering will be conferred in May 2006.